VYSOKÉ UČENÍ TECHNICKÉ V BRNĚ

BRNO UNIVERSITY OF TECHNOLOGY

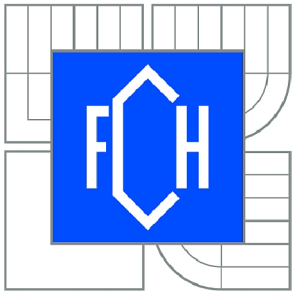

FAKULTA CHEMICKÁ

ÚSTAV CHEMIE MATERIÁLŮ

FACULTY OF CHEMISTRY

INSTITUTE OF MATERIALS SCIENCE

MOLECULAR MODELLING - STRUCTURE AND PROPERTIES OF CARBENE-BASED CATALYST

MOLEKULOVÉ MODELOVÁNÍ - STRUKTURA A VLASTNOSTI KATALYZÁTORŮ NA BÁZI KARBENŮ

BAKALÁŘSKÁ PRÁCE

BACHELOR'S THESIS

AUTOR PRÁCE — EVA KULOVANÁ

AUTHOR

VEDOUCÍ PRÁCE — RNDr. LUKÁŠ RICHTERA, Ph.D.

SUPERVISOR

BRNO 2010

Vysoké učení technické v Brně
Fakulta chemická
Purkyňova 464/118, 61200 Brno 12

Zadání bakalářské práce

Číslo bakalářské práce:	**FCH-BAK0439/2009**	Akademický rok: **2009/2010**
Ústav:	Ústav chemie materiálů	
Student(ka):	**Eva Kulovaná**	
Studijní program:	Chemie a chemické technologie (B2801)	
Studijní obor:	Chemie, technologie a vlastnosti materiálů (2808R016)	
Vedoucí práce	**RNDr. Lukáš Richtera, Ph.D.**	
Konzultanti:		

Název bakalářské práce:

Molekulové modelování - struktura a vlastnosti katalyzátorů na bázi karbenů

Zadání bakalářské práce:

Pomocí programu ArgusLab, případně i s využitím dalšího softwaru umožňujícího molekulové modelování, budou vytvořeny modely několika konkrétních karbenových sloučenin, bude provedena jejich geometrická optimalizace a vypočítány některé dostupné vlastnosti (UV/Vis spektra), případně napredikována IR, RA a NMR spektra. Z optimalizovaných struktur již známých sloučenin budou zjištěny vazebné úhly a vazebné vzdálenosti a tato data budou srovnána s daty získanými z CCDC (Cambridge Crystallographic Data Centre).

Termín odevzdání bakalářské práce: 28.5.2010

Bakalářská práce se odevzdává ve třech exemplářích na sekretariát ústavu a v elektronické formě vedoucímu bakalářské práce. Toto zadání je přílohou bakalářské práce.

Eva Kulovaná Student(ka)	RNDr. Lukáš Richtera, Ph.D. Vedoucí práce	prof. RNDr. Josef Jančář, CSc. Ředitel ústavu

V Brně, dne 1.12.2009

prof. Ing. Jaromír Havlica, DrSc.
Děkan fakulty

ABSTRACT

Molecular modelling enables to predict behaviour of the new compounds and helps to interpret experimental data. The objective of our study was the prediction of selected properties of polymerization catalysts based on carbenes, the prediction of their structures and spectral characteristics.

To confirm the behaviour of carbenes and their precursors based on chlorides selected characteristics of a molecule were studied. The visualization of selected molecular orbitals and electrostatic potential-mapped electron density surface was made. Subsequently, bond distances and bond angles of selected imidazole and imidazoline compounds and from them prepared "free" carbenes were obtained by using computer programs. Data of structural similar compounds, which have been already characterized, were obtained from CCDC (Cambridge Crystallographic Data Centre) and were compared with our calculated data. Infrared (IR) and Raman spectra of the imidazole salt and the infrared spectrum of the appropriate carbene were measured. The spectra measured were compared with predicted spectra.

ABSTRAKT

Molekulové modelování umožňuje předpovídat chování nových látek a napomáhá při jinak obtížné interpretaci experimentálních dat. Záměrem našeho studia byla predikce vybraných vlastností polymeračních katalyzátorů na bázi karbenů, predikce jejich struktur a spektrálních charakteristik.

K ověření chování karbenů a jejich prekurzorů ve formě chloridů byly studovány vybrané charakteristiky molekuly. Byla provedena vizualizace vybraných molekulových orbitalů a map elektrostatických potenciálů a elektronových hustot. Následně pomocí počítačových programů byly získány teoretické vazebné délky a úhly vybraných imidazolových a imidazolinových sloučenin a z nich připravených karbenů. Data strukturně podobných, již charakterizovaných sloučenin, byla získána z CCDC (Cambridge Crystallographic Data Centre) a následně konfrontována s námi vypočítanými daty. Byla změřena infračervená (IČ) a Ramanova spektra imidazolové soli a IČ spektrum příslušného karbenu. Tato spektra byla konfrontována s napredikovanými.

KEYWORDS

N-heterocyclic carbenes, *ab initio* methods, DFT methods, IR spectroscopy, Raman spectroscopy

KLÍČOVÁ SLOVA

N-heterocyclické karbeny, *ab initio* metody, DFT metody, IČ spektroskopie, Ramanova spektroskopie

KULOVANÁ, E. *Mollecular modelling – structure and properties of carbene-based catalysts.* Brno: Vysoké učení technické v Brně, Fakulta chemická, 2010. 62 p. Vedoucí bakalářské práce RNDr. Lukáš Richtera, Ph.D.

DECLARATION

I declare that the diploma thesis has been worked out by myself and that all the quotations from the used literary sources are accurate and complete. The content of diploma thesis is the property of the Faculty of Chemistry of Brno University of Technology and all commercial uses are allowed only if approved by both the supervisor and the dean of the Faculty of Chemistry, BUT.

.....
student‘s signature

Acknowledgments

I would like to thank RNDr. Lukáš Richtera and Ph.D., Mgr. Soňa Hermanová, Ph.D. for valuable advice and comments.

Contents

1 Introduction

Molecular modelling has made a significant progress together with the development of the computer technology. It uses the results of theoretical chemistry as inputs into efficient computer programs to calculate the structures and properties of molecules. First, computational quantum chemistry has been developed. The advancement of computer softwares has continued in many research groups. In 1998 John Pople, who made the methods more efficient and made their application more popular, was awarded the Nobel Prize[1].

On the basis of *ab initio* methods, which were proved to be competent for the prediction of molecular geometry, the carbene (methylene) intermediate has been studied. Nowadays, the accuracy of these methods is similar or better to that of most experimental methods[1].

2 Theoretical part

2.1 Divalent carbon

Carbon is the fourth most abundant chemical element in the universe by mass. It forms around 14 millions of different compounds. Besides its occurrence in all known life carbon is the basis of organic compounds. It can form hydrocarbons or many other groups of important biological compounds. Mostly, the carbon is tetracoordinate or tricoordinate (number of its nearest neighbours) and tetravalent (four electrons are available to form covalent bonds). Thus there is often relationship between coordination number and the valence. Carbon is known with all coordination numbers[1] from 0 to 8.

Chemistry of high-coordinate carbon which can be involved in organometallic compounds has been investigating for about a century. Unlike carbon atoms transition metal atoms can possess low-lying d-orbitals. Carbon almost forms four covalent, *i.e.* two-centre two-electron (2c-2e) bonds oriented to the corners of a tetrahedron. High-coordinate carbon compounds can be classified into electron-deficient and electron-rich classes. Most high-coordinate carbon compounds are electron-deficient, having three-centre two-electron (3c-2e) bonds[3]. These compounds have eight electrons formally predicable around the central carbon. The characteristic compound with a pentacoordinate carbon is methonium cation. Its structure can be described by three standard 2c-2e bonds and a 3c-2e bond[4]. In Fig. 1 pentacoodinate, hexacoordinate and heptacoordinate carbon is depicted.

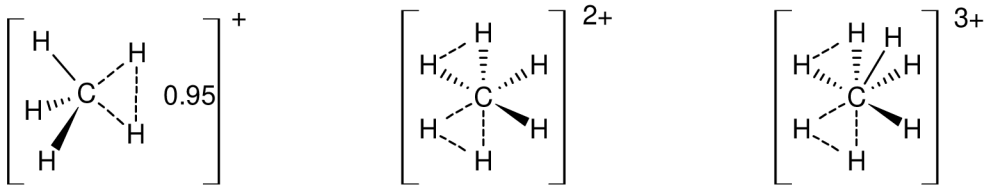

Fig. 1 Electron-deficient high-coordinate carbon

On the other hand electron-rich pentacoordinate carbon compounds have ten electrons formally predicable around the central carbon and include a three-centre four-electron (3c-4e) bond. The formation of a three-centre four-electron 3c-4e bond is called "hypervalent" bonding system and involves an apical bond of a pentacoordinate trigonal bipyramidal molecule[5]. To experimentally creation of a 3c-4e bond three types of an interation can be considered: an interaction a pair of unshared electrons in a p orbital with two free radicals (Fig. 2a), an interaction of a vacant 2p orbital of the central carbon atom with two lone-pair electrons (four electrons) (Fig. 2b) or an interaction between a vacant C–X σ* orbital and a lone pair of a nucleophile (Fig. 2c). In some cases, the hypervalent pentacoordinate carbon can be found as the transition state of S_N2 reactions (Fig. 3)[6].

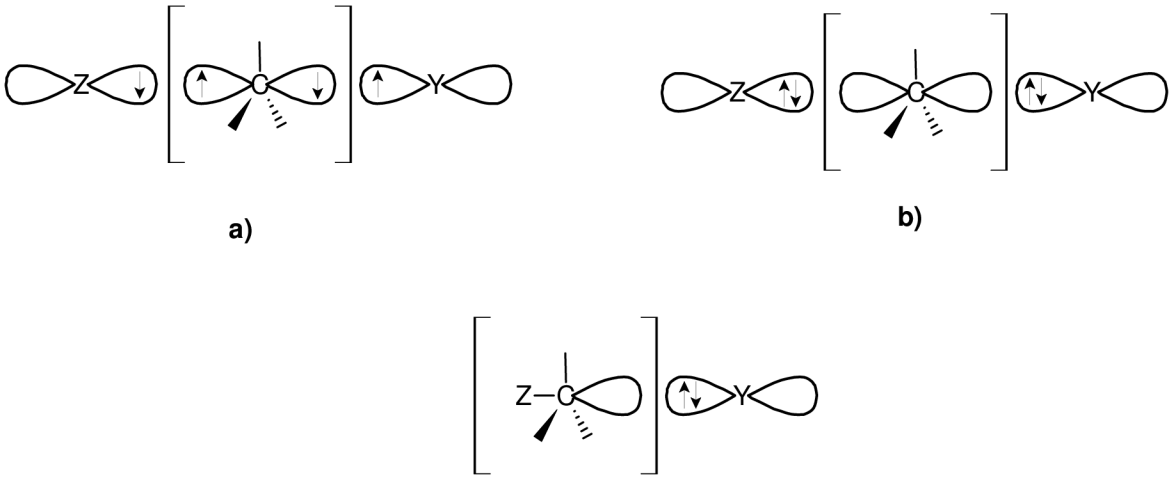

Fig. 2 Formation of three-centre four-electron bond of pentacoordinate carbon

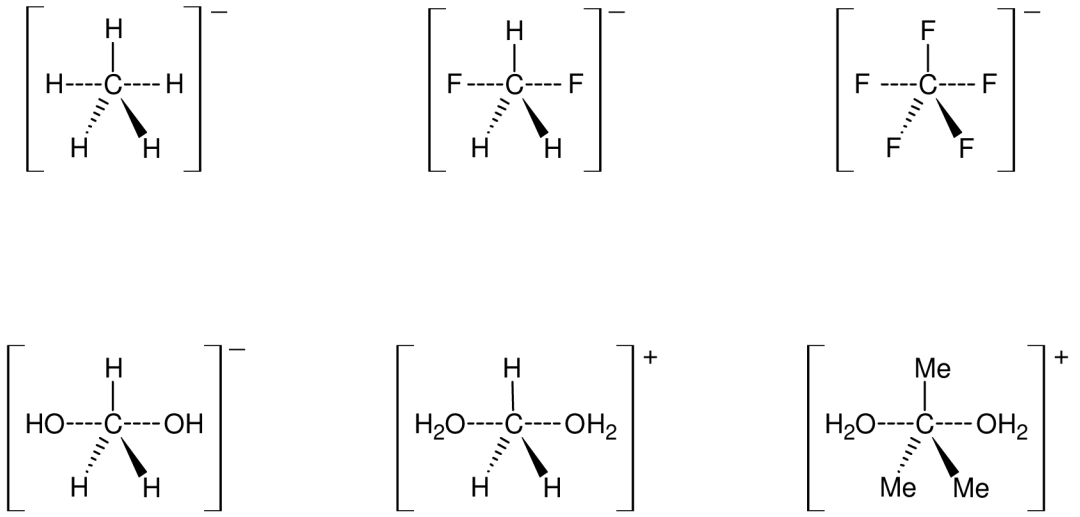

Fig. 3 Hypervalent pentacoordinate carbon of transition state of S_n2

Some persistent free radicals as tris(2,4,6-trichlorophenyl)methyl radical include trivalent carbon. The stabilization of a radical is largely because of delocalization of the unpaired electron, whereas persistence is mainly because of steric hindrance of the substituents around trivalent carbon[7].

Some unusual compounds can contain divalent carbon as well (its coordination number equals two). Our study will be focused on carbenes, which contain that carbon.

2.2 Definition and classification of carbenes

Carbenes are neutral compounds containing a divalent carbon with only six valence electrons and having general formula RR´C**:** (Fig. 4). Generally, carbenes are classified into two groups: singlet and triplet carbenes differing significantly in chemical reactivity pattern. Singlet carbenes behave like zwitterions (will be discussed in Section 2.4.2). Triplet carbenes

participate in chemical reactions similarly like free radicals. Most carbenes have a nonlinear triplet ground state; however they have very short life-time. The simplest carbene is H_2C**:** also called methylene.

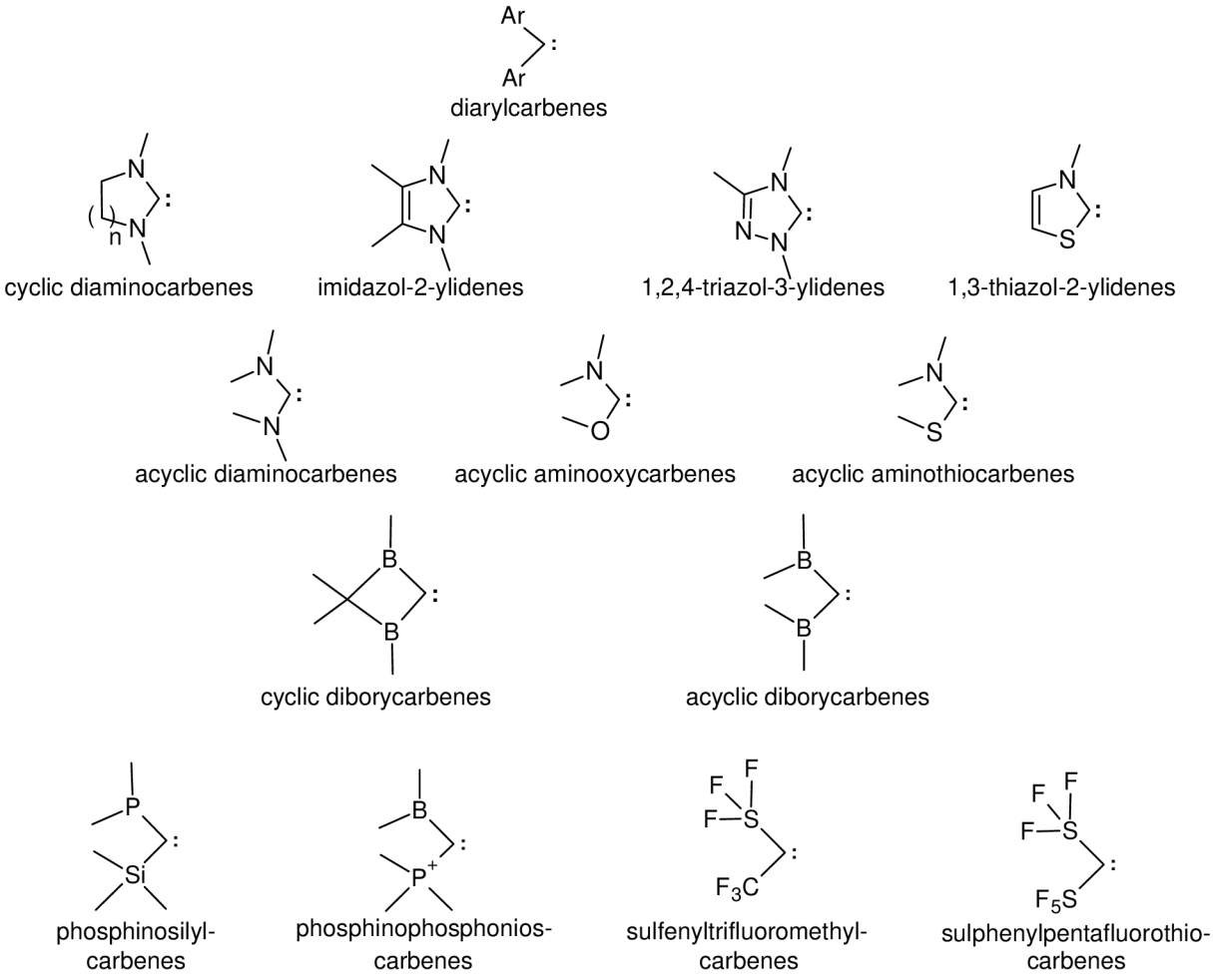

Fig. 4 Known types of carbenes

Carbenes have been known as ligands in transition metal complexes chemistry as well. From this point of view the transitional metal carbene complexes can be clasified into two types: Fischer and Schrock carbenes. The Fischer carbenes are electrophilic at the carbene carbon atom and they are in singlet state. On the other hand, the Schrock ones have more nucleophilic carbene centre atoms.

Heterocyclic carbenes contain at least one atom of carbon and at least one atom of other element, such as oxygen, sulphur or nitrogen in a ring structure. Heteroatom donor groups on carbene center render the originally degenerate orbitals on carbon unequal in energy, thus enhance the nucleophilicity of the carbon atom and thermodynamic stability. Although several combinations of heteroatoms in carbene ring are possible, until 1997 only singlet carbenes with two nitrogen atoms were isolated as crystalline compounds[8].

2.3 History

Chemistry of carbenes was established in the 1950s by Skell[9]. Fischer et al. [10] introduced carbenes into inorganic and organometallic chemistry in 1964. Afterwards, metal complexes with carbenes ligands became important in organic synthesis, catalysis and macromolecular chemistry[11] and hence chemistry of heterocyclic carbenes began to progress. Since the objective of the thesis deals with N-heterocyclic carbenes structures, the review will be focused on carbenes having nitrogen atoms in the ring. These compounds were studied by Wanzlick et al.[12] in the early 1960s, unfortunately without the possibility of "free" isolable N-heterocyclic carbenes preparation. Arduengo et al.[13] succeed in preparation of free carbene by deprotonation of imidazolium ion (Fig. 5) in 1991.

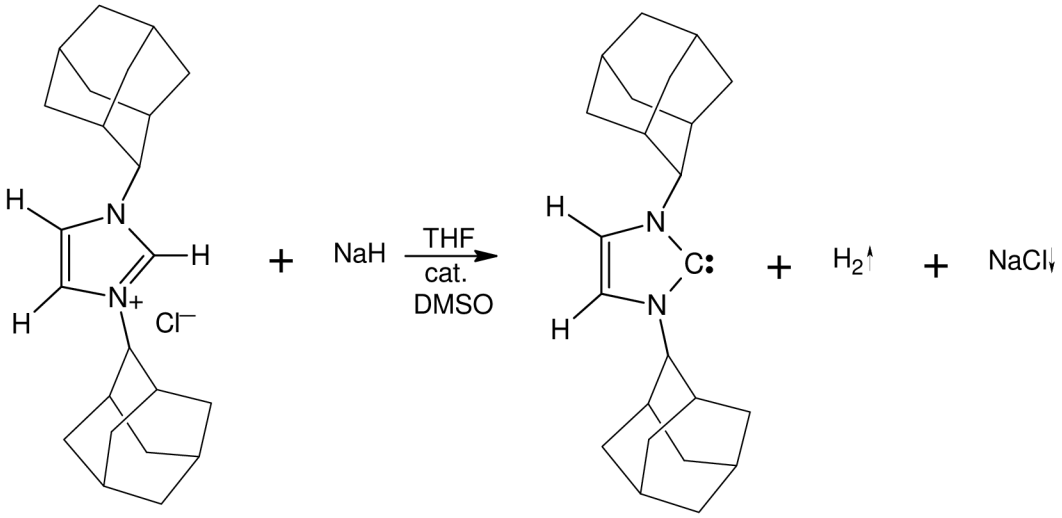

Fig. 5 Deprotonation of imidazolium ion

2.4 Ground-state spin multiplicity

The spin multiplicity M is defined as:

$$M = 2S + 1 \qquad (2.4\text{-}1)$$

where S is total spin quantum number[17]. The system with M = 1 is called a singlet state, because it has exactly one possible state. A system with M = 2 is called a doublet state and with M = 3 is called a triplet state and so on. For example the molecule in Fig. 7a is in the triplet state, because the spin multiplicity equals three ($M = 2\times½\times2 + 1 = 3$). On the other hand the molecule in Fig. 7d contains two opposite spins, so it is in a singlet state, because the spin multiplicity equals one ($M = 2\times½\times2 + 1 = 1$).

Carbon atom in carbenes can be either linear or bent. Each geometry can be described by a certain degree of hybridization. The linear geometry contains an sp-hydridized carbene center with two nonbonding degenerate orbitals (p_x and p_y). Whereas bent geometry contains an sp^2-hybridized carbene center, the p_y orbital is almost unchanged (usually called p_π), while p_x orbital is stabilized since it gets some s character (therefore called σ) (Fig. 6). Most carbenes are bent and their frontier orbitals are called σ and p_π.

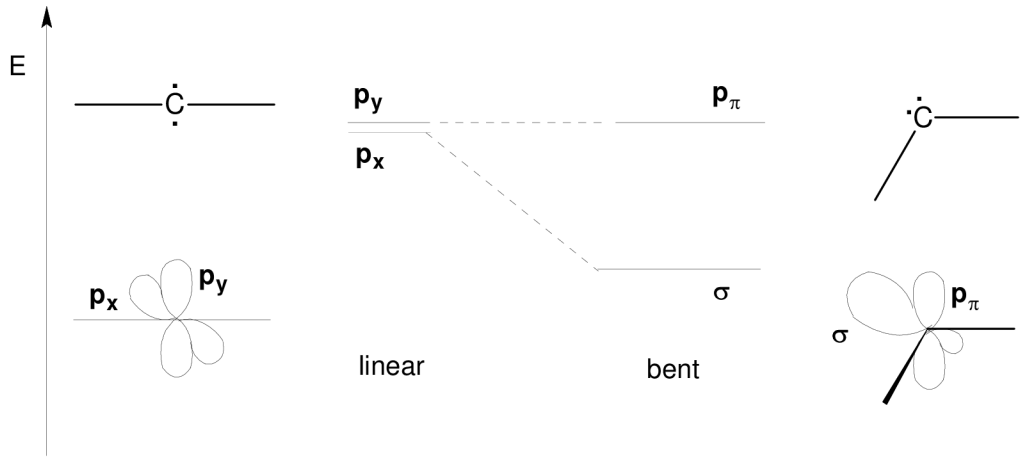

Fig. 6 Relationship between the carbene bond angle and the nature of the frontier orbitals

Four electronic configurations of carbenes can exist (Fig. 7). The left upper index denotes the spin multiplicity. The right lower index and the symbols A and B are related to point groups and the symmetry. The symbol A is common used, when rotation around the principal axis is symmetrical, whereas the symbol B is common used, when rotation around the principal axis is asymmetrical. The two nonbonding electrons can be in two different orbital with parallel spins (triplet state). The molecule, marked **a)** in Fig. 7, is correctly described by the $\sigma^1 p_\pi^1$ configuration ($^3B_1$ state). On the other hand for singlet carbenes the two nonbonding electrons can be paired in the same σ or p_π orbital. Therefore, there are two different singlet states ($^1A_1$ states), the σ^2, marked **b)**, being more stable than the p_π^2, marked **c)**. Last, an excited singlet state with $\sigma^1 p_\pi^1$ configuration is called $^1B_1$ state and it is denoted as **d)**[14].

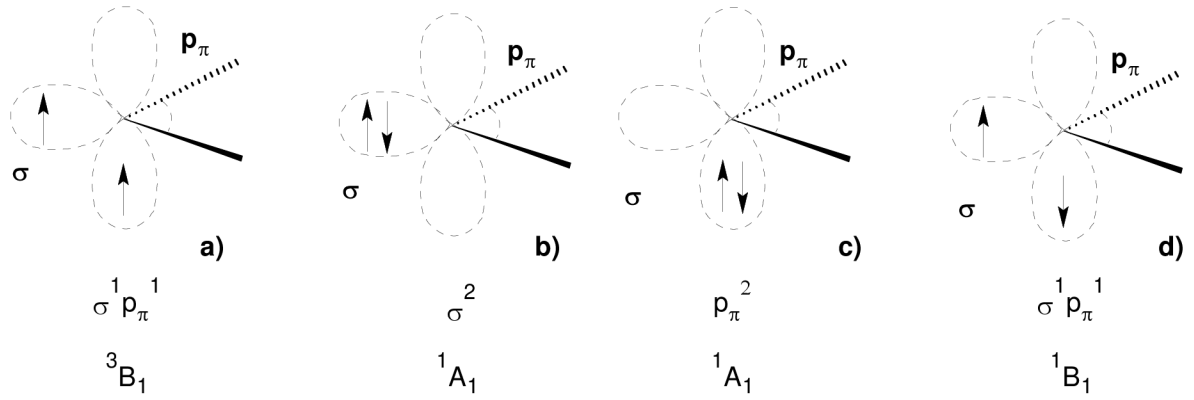

Fig. 7 Electronic configurations of carbenes

The determination of carbene state multiplicity and energy gap between singlet and triplet is important for understanding the carbene reactivity. Thus, the ground-state multiplicity is a crucial feature of carbenes since it dictates their reactivity[15]. Singlet carbenes have a filled and a vacant orbital. Whereas triplet carbenes have two singly occupied orbitals and they are generally treated as diradicals. The triplet carbenes can not be stabilized through thermodynamic effects; they have to be rendered unreactive by steric protection.

The carbene ground-state multiplicity is related to the relative energy of the σ and p_π orbitals. Gleiter and Hoffmann determined that a σ-p_π gap of at least $3.2 \cdot 10^{-22}$ kJ (2 eV) is necessary to impose a singlet ground state, whereas a value below $2.4 \cdot 10^{-22}$ kJ (1.5 eV) leads to a triplet ground state[16].

2.4.1 Inductive effects

The inductive effect is an experimentally observable effect of the transmission of charge through a chain of atoms by electrostatic induction[17]. The electron cloud in a σ-bond between two different atoms is not equal and is slightly displaced towards the more electronegative of the these atoms. The more electronegative atom has a partial negative charge (δ^-) and the another atom has a partial positive charge (δ^+). If the electronegative atom is bonded to a chain of atoms, usually carbon, the positive charge is relayed to the other atoms in the chain. This is the electron-withdrawing inductive effect (-I effect). Some groups are less electron-withdrawing than hydrogen and are regarded as electron-donating (+I effect)[18].

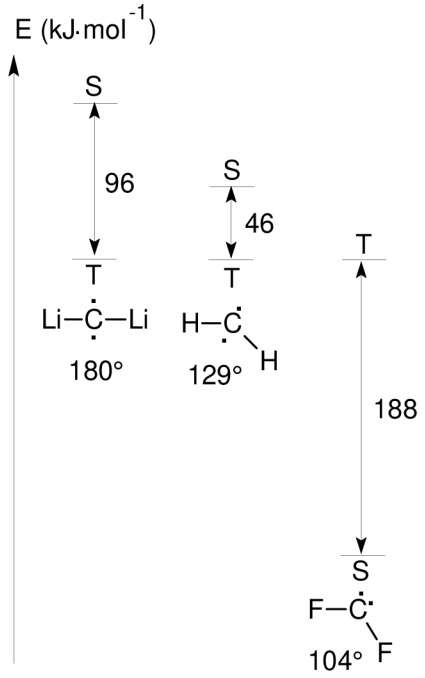

Fig. 8 Influence of the substituents' electronegativity on the ground state carbene multiplicity

Inductive effect has the influence of multiplicity on the carbene, σ-electron-withdrawing substituents favour the singlet versus the triplet state. In particular, Harrison et al.[19] showed that the ground state goes from triplet to singlet when the substituents are changed from electropositive lithium to hydrogen and to electronegative fluorine (although mesomeric effects surely also plays role for the latter element) (Fig. 8).

The σ nonbonding orbital is inductively stabilized by σ-electron-withdrawing substituents, that is why its s character increase, whereas the p_π orbital is unchanged. The singlet state is favoured, because the σ-p_π gap is increased. In contrast, σ-electron-donating substituents induce a small σ- p_π gap which favours the triplet state[14].

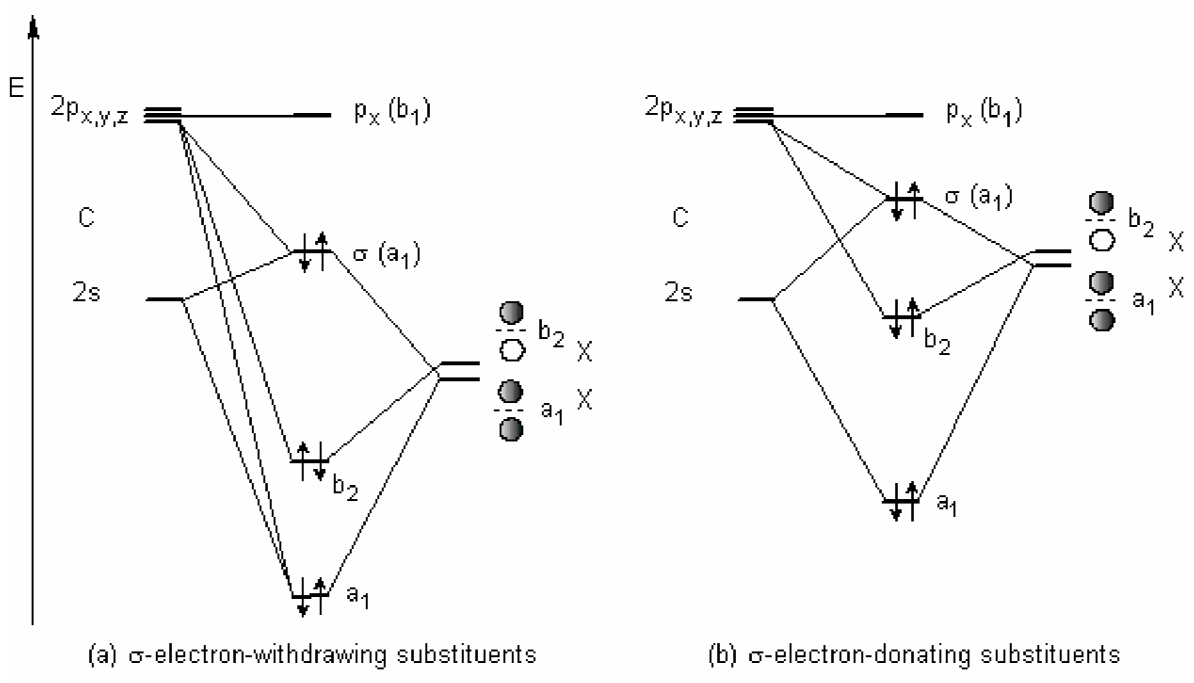

Fig. 9 Diagrams showing the influence of the inductive effects

2.4.2 Mesomeric effects

The mesomeric or resonance effect is attributed to a substituent due to overlap of its p- or π-orbitals with the p- or π-orbitals of the rest of the molecular entity. The effect is symbolized by the letter **M**. The mesomeric effect is negative (**-M**) when the substituent is an electron-withdrawing group and the effect is positive (+**M**) when the substituent is an electron-donating group[17].

Mesomeric effects can play a more important role[20], although inductive effects dictate the ground-state multiplicity of a few carbenes. Substituents interacting with the carbene centre can be divided into two types, namely X (for π-electron-donating groups such as –F, –Cl, –Br, –I, $–NR_2$, –OR, –SR, $–SR_3$, …) and Z (for π-electron-withdrawing groups such as –COR, –CN, $–CF_3$, $–BR_2$, $–SiR_3$, –PR, …). The singlet carbenes can be classified according to their substituents: the highly bent (X,X)-carbenes and the linear or quasi-linear (Z,Z)- and (X,Z)-carbenes. In all cases, the mesomeric effects comprise the interaction of the carbon orbitals (s, p_π or p_x, p_y) and appropriate p or π orbitals of two carbene substituents (Fig. 10)[14].

(X,X)-Carbenes marked as (a) in Fig. 10 are predicted to be bent singlet carbenes[21]. The energy of the vacant p_π orbital is increased by interaction with the symmetric combination of the substituent lone pairs which is marked (b_1). As the σ orbital stays almost unchanged, the σ-p_π gap is increased and the singlet state is favoured. Nonsymmetric combination of the substituent lone pairs is marked (a_2) and is close in energy to σ orbital. Donation of the X-substituent lone pairs results in a polarized four-electron three-center π-system. The C-X bonds get some multiple bond character, so (X,X)-carbenes are best described by the superposition of two zwitterionic structures with a negative charge at the carbene center. The most representative carbenes of this type are the transient dimethoxy-, dihalocarbenes and the stable diaminocarbenes[14].

Most of the (Z,Z)-carbenes are predicted to be linear singlet carbenes[21,22]. As depicted in Fig. 10b, the symmetric combination of the substituent vacant orbitals interacts with the p_y

orbital. This interaction does not have influence on the p_x orbital. Therefore, the (p_x, p_y) degeneracy is broken. These carbenes have a singlet ground state although they are linear[21]. This substitution pattern results in a polarized two-electron three-center π-system. Here also, the C-Z bonds have some multiple bond character, so these (Z,Z)-carbenes are best described by superposition of two zwitterionic structures featuring a positive charge at the carbon atom. Some of the most studied carbenes of this type are transient dicarbomethoxycarbenes and "masked" diborylcarbenes[14].

Last, the quasi-linear (X,Z)-carbenes combine both types of electronic interaction. (Fig. 10c) marks interaction of the X substituent lone pair with the p_y orbital, while the Z substituent vacant orbital interacts with the p_x orbital. These substituent effects favour the singlet state (the vacant p_y orbital is destabilized, while the filled p_x orbital is stabilized). These two interactions result in a polarized allene-type system with XC and CZ multiple bonds. Appropriate examples of this type of carbene represent transient halogenocarboethoxycarbenes and the stable phosphinophosphoniocarbenes and phosphinosilylcarbenes[14].

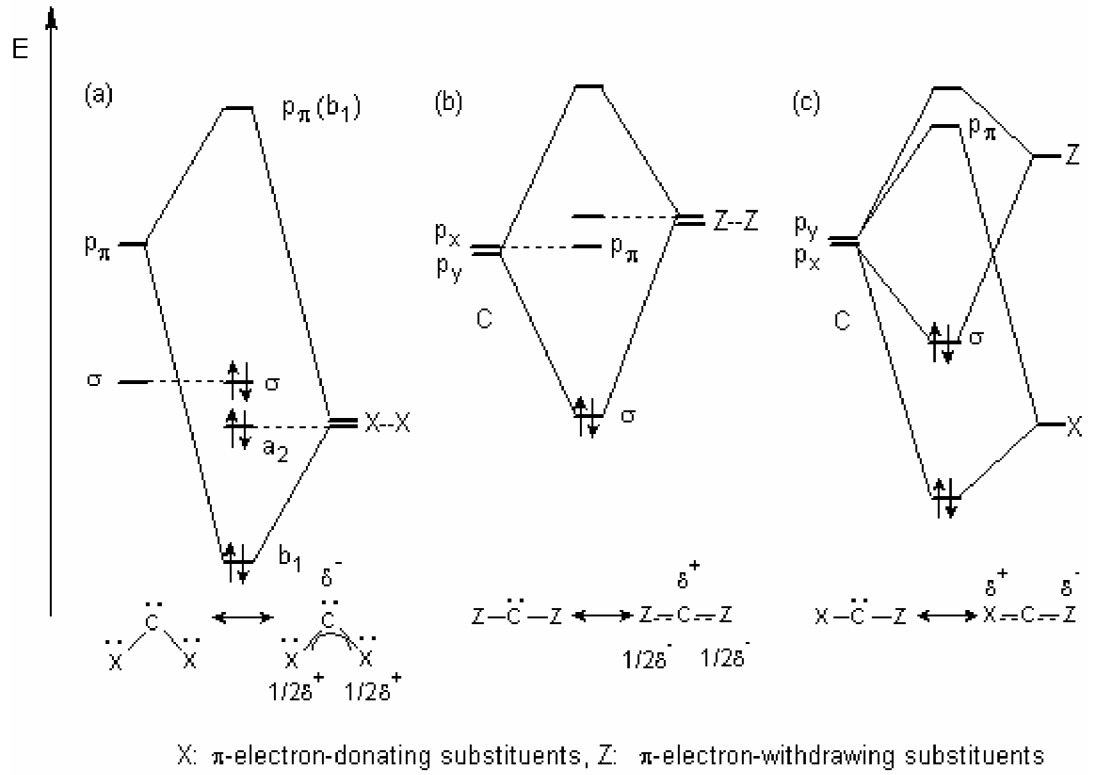

Fig. 10 Pertubation orbital diagrams showing the influence of the mesomeric effects

2.4.3 Steric effect

Steric effects are based on the fact that each atom within a molecule occupies a certain amount of space. If atoms are brought too close together, there is an associated cost in energy due to overlapping electron clouds. Consequently this effect can influence the preferred shape of molecules (conformation) and reactivity as well.

All types of carbenes are kinetically stabilized by bulky substituents. Moreover, if electronic effects are negligible, the steric effects can dictate the ground-state spin

multiplicity[14]. A linear geometry will favour the triplet state, so the carbene bond angle has the influence on the ground-state spin multiplicity. The increase in the steric bulk of carbene substituents broadens the carbene bond angle and therefore the triplet state is favoured[23].

2.5 N-heterocyclic carbenes

We can classify N-heterocyclic carbenes as (X,X)-Carbenes. Among them 4 types of stable N-heterocyclic carbenes are recognized: imidazol-2-ylidenes, imidazolin-2-ylidenes, 1,2,4-triazol-3-ylidenes and 1,3-thiazol-2-ylidenes (Fig. 11). For many purpose they are best described by resonance forms B and C, which may be summarized by structure D or E in case of imidazol-2-ylidenes (Fig. 12).

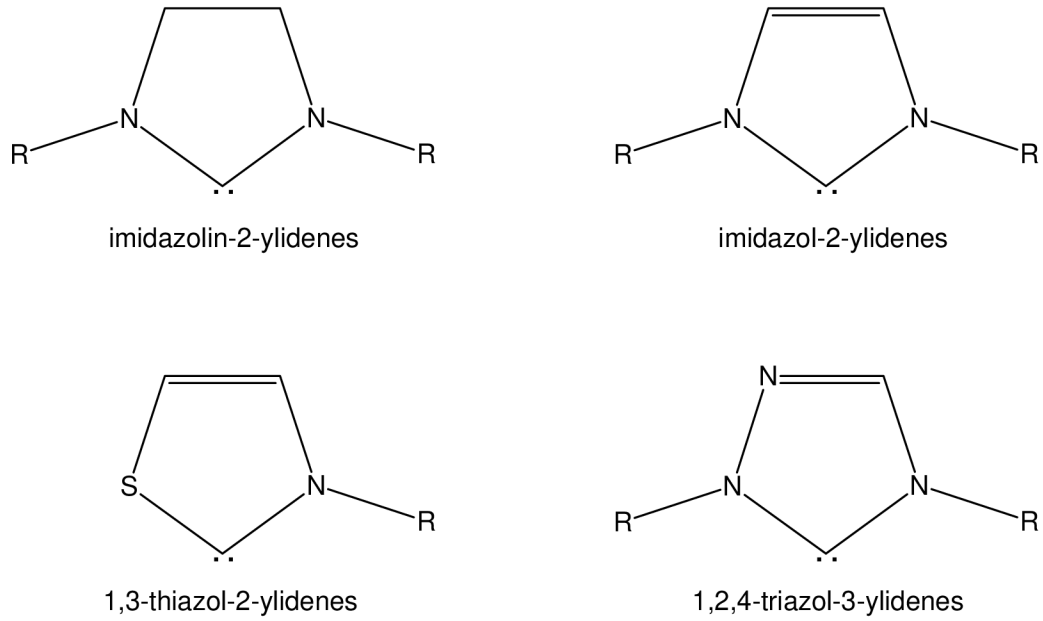

Fig. 11 Types of stable N-heterocyclic carbenes

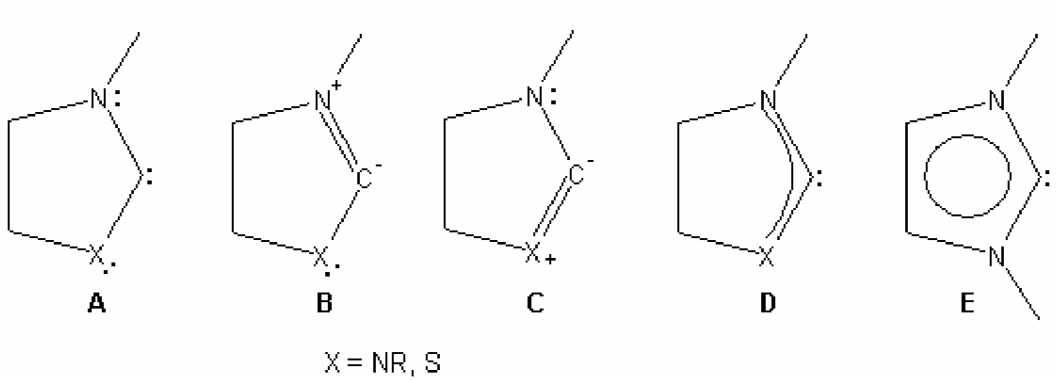

Fig. 12 Resonance structures of N-heterocyclic carbenes

N-heterocyclic carbenes could be synthesized by number of ways, for example by deprotonating of imidazolium salts[13] (Fig. 5), by thermal elimination of methanol with 5-methoxy-1,3,4-triphenyl-4,5-dihydro-1H-1,2,4-triazol (Fig. 13a) or by reduction of thiones with potassium in boiling THF[14] (Fig. 13b).

The carbenes that can be isolated as stable crystalline compounds at room temperature are also known as Arduengo carbenes. N-heterocyclic carbenes are often colourless crystals thermodynamically stable in the absence of oxygen and moisture[13]. On the other hand some carbenes are stable only in solution[24].

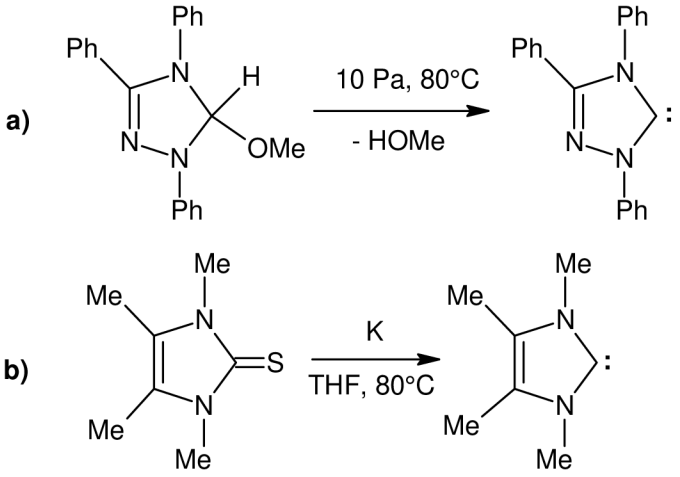

Fig. 13 The examples of the synthesis of N-heterocyclic carbenes

2.5.1 Properties

N-heterocyclic carbenes have a pronounced low-energy HOMO (highest occupied molecular orbital) and a high-energy LUMO (lowest unoccupied molecular orbital)[25]. Due to a small HOMO-LUMO gaps carbenes are very reactive. They are stronger electron-pair donors than amines due to the lower electronegativity of carbon atom. Their electron-accepting capabilities are more significant than that of boranes. These compounds benefit from a "push-pull" effect, because the amino groups are π-donating (mesomeric) and σ-withdrawing (inductive)[8].

The extent of stability and aromaticity (for 6π -electron systems) of free carbenes and their homologues depends on the point of view. The aromatic compounds must fulfil following conditions:

1. coplanar structure-all atoms must be localized in the same plane
2. a delocalized conjugated π-system
3. a number of π delocalized electrons must be 4n + 2 (Hückel's rule).

The stability of these compounds results from electronic effects (mesomeric +M as well as inductive -I effects), although steric hindrance plays an important role as well. In the imidazol-2-ylidenes the nitrogen lone pairs and the C=C double bonds ensure the kinetic stability because of their high electron density, but π-donation by nitrogen lone pairs plays a minor role. The aromatic character of these carbenes is less pronounced than that of imidazolium salts precursors, but it brings an additional stabilization of ~ 109 kJ·mol^{-1} (~ 26 kcal·mol^{-1})[26].

Generally, for preparative chemistry the kinetic stability of compounds is crucial. Stable N-heterocyclic carbenes are being studied for several reasons. Structure, reactivity and theoretical understanding of these highly Lewis basic (one of the strongest known bases) and nucleophilic molecules are interest. Moreover, stable "ylidene" carbenes are used for

preparation of main group and transitional metal complexes. However several "in situ" methods for syntheses metal "ylidene" complexes without the necessity of free carbenes or their equivalents isolation have been developed as well[8].

2.5.2 N-heterocyclic carbenes as nucleophilic catalysts

A nucleophile is a reagent which forms a chemical bond to the electrophile by donating both bonding electrons. All molecules or ions with a free pair of electrons can act as nucleophiles, therefore N-heterocyclic carbenes belong to nucleophilic catalysts and have various catalytic applications in nature as well as in synthetic chemistry[8]. Some of these compounds found catalytic applications in organic synthesis, for example in the formoin condensation reactions affording C2 to C6 carbohydrates, in oxidative benzoin condensation of aldehydes, alcohols and aromatic nitro compounds to yield esters, in the Michael-Stetter reaction yielding 1,4-dicarbonyl derivatives and in the benzoin condensation of aldehydes to α-hydroxyketones[27] (Fig. 14). Chiral triazolium salts as catalyst precursors are used in asymmetric variants of ylidene-catalyzed benzoin condensations and Michael-Stetter reaction[28]. N-heterocyclic carbenes can catalyze ring-opening polymerization as well[29] (Fig. 15).

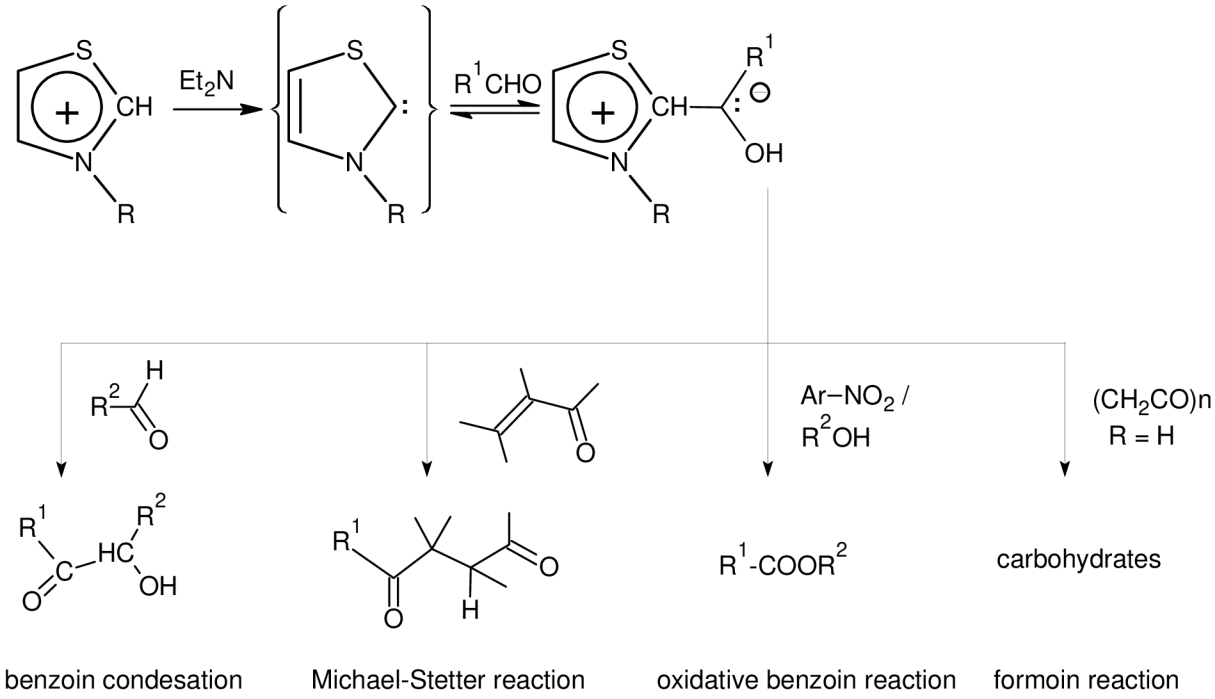

Fig. 14 Organic transformations of aldehydes catalysed by N-heterocyclic ylidenes

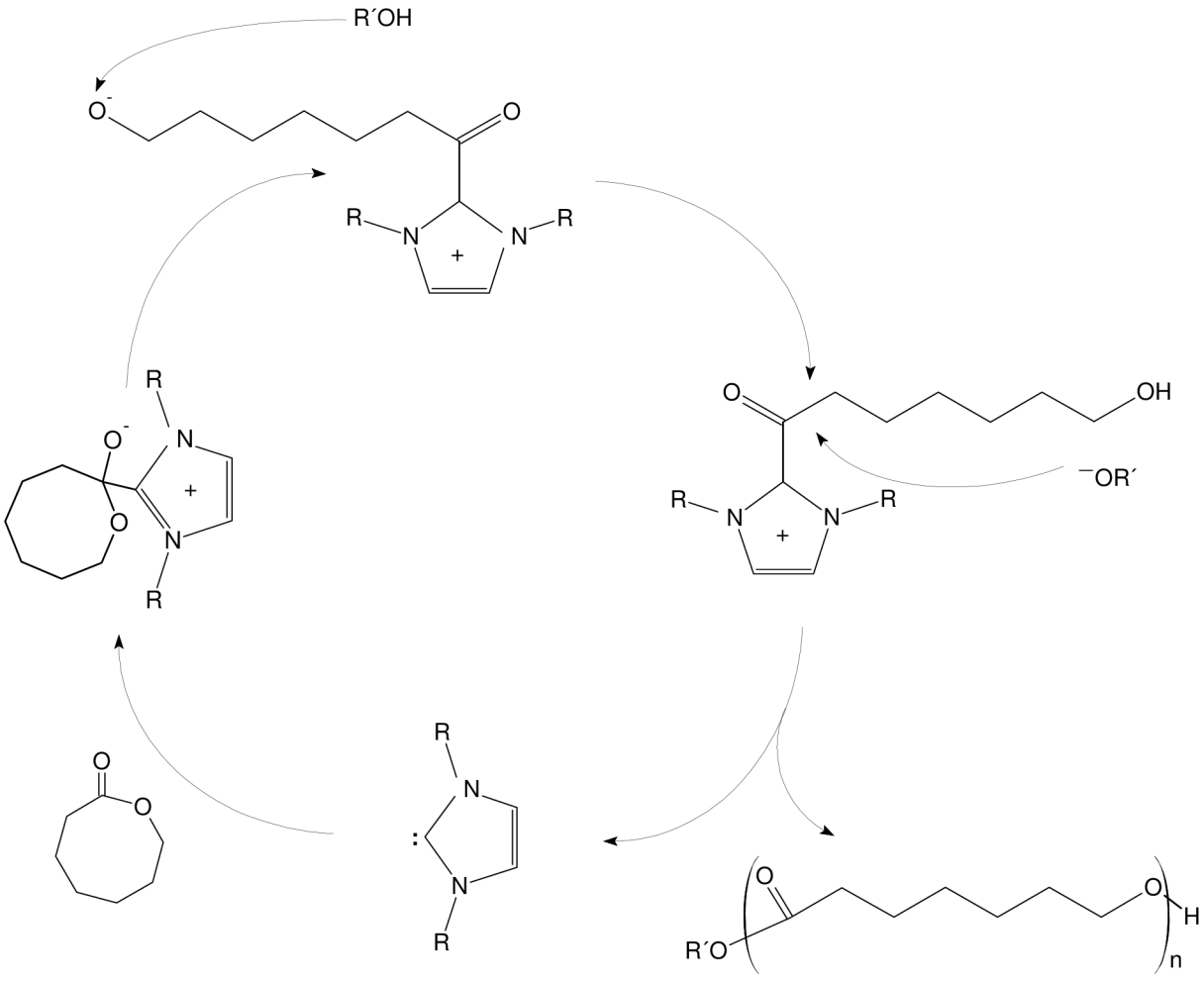

Fig. 15 Ring-opening polymerization catalyzed by N-heterocyclic carbenes

2.5.3 N-heterocyclic carbenes as bases

Some N-heterocyclic carbenes can form stable adducts with soft or weak Lewis acids, in which they act as pronouncedly basic σ donors. Electron density at carbene centre decrease upon complexation to a Lewis acid and ylidic mesomeric structures become more important. Heteroaromatic imidazolium salts are adducts of the free carbene with the strongest Lewis acid, a proton[8].

2.5.3.1 Lewis concept of acids and bases

A Lewis base acts as an electron-pair donor that has a lone pair of electrons in the HOMO, whereas a Lewis acid has alone orbitals of low energy LUMO and it can accept electrons. Some examples of Lewis acids are:

1. metal cations complexed by ligands
2. electrophiles (attracking Lewis acid)
3. electrofuges (Lewis acid leaving group)
4. classic electron deficient species such BF_3 and $AlCl_3$
5. cationic spectator counter ions (cations are unchanged during the reaction)
6. electron deficient π-systems which take part in multicentre interactions

Some examples of Lewis bases are:

1. anions
2. proton abstractors
3. conjugate Brønsted bases
4. nucleophiles
5. nucleofuges
6. ligands
7. anionic counter ions
8. electron-rich π-systems[30]

2.5.3.2 Pearson concept of acids and bases

In 1963, the HSAB concept (hard and soft acid and bases) was introduced by Pearson[31]. According this theory *soft* acids react faster and form stronger bonds with *soft* bases. On the other hand *hard* acids react faster and form stronger bonds with *hard* bases. Hard acids and hard bases tend to have:

1. small atomic/ionic radiuc
2. high oxidation state
3. low polarizability
4. high electronegativity
5. energy low-lying HOMO (bases) or energy high-lying LUMO (acids).

On the other hand soft acids and soft bases tend to have:

1. large atomic/ionic radius
2. low or zero oxidation state
3. high polarizability
4. low electronegativity
5. energy high-lying HOMO (basis) and energy-low lying LUMO (acid)[32].

Tab. 1 Hard and soft acid and bases

Acids				**Bases**			
hard		**soft**		**hard**		**soft**	
hydronium	H^+	mercury	CH_3Hg^+, Hg^{2+}, Hg_2^{2+}	hydroxide	OH^-	hydride	H^-
alkali metals	Li^+, Na^+, K^+	platinum	Pt^{2+}	alkoxide	RO^-	thiolate	RS^-
titanium	Ti^{4+}	palladium	Pd^{2+}	halogens	F^-, Cl^-	halogens	I^-
chromium	Cr^{3+}, Cr^{6+}	silver	Ag^+	ammonia	NH_3	phosphine	PR_3
boron trifluoride	BF_3	borane	BH_3	carboxylate	CH_3COO^-	thiocyanate	SCN^-
carbocation	R_3C^+	P-chloranil		carbonate	CO_3^{2-}	carbon monoxide	CO
		bulk metals	M^0	hydrazine	N_2H_4	benzene	C_6H_6
		gold	Au^+				

2.6 Molecular modelling

Molecular modelling made fast progress with development in the computing and today it is a necessary part of research in many research laboratories. It enables to predict the behaviour of the new compounds and helps to interpret experimental data. The term "*in silico*" is used for research using computer calculations and simulations. Today we can classify methods of molecular modelling into 3 groups - molecular mechanics, quantum mechanics and simulation methods. In principle simulation methods use both quantum mechanics and molecular mechanics, so they will not be discussed.

For molecular modelling terms as "theoretical chemistry" or "computational chemistry" are used. "Theoretical chemistry" is often considered synonymous with quantum mechanics. On the other hand, the term "computational chemistry" includes quantum mechanics as well as molecular mechanics, simulations, conformational analysis and other computer-based methods. Molecular modellers use all of these methods[33].

2.6.1 Coordinate systems

Specification of the position of atoms or molecules in the system to a modelling program is one of the most important point in molecular modelling. We can use two common ways. The simpler way is to specify to *Cartesian coordinates* of all atoms present. Many programs can generate these coordinates. The second way is using of *internal coordinates*, in which the position of each atom is described relative to other atoms in system. These coordinates are usually written as a Z-matrix. They describe the relationship between all atoms in a single molecule[33].

2.6.2 Potential energy surfaces

With using of the Born-Oppenheimer approximation, which will be discussed in Section 2.7.5, we can separate the electronic and nuclear motions. We can consider the energy of a molecule in its ground electronic state as a function of the nuclear coordinates only because of much smaller mass of electrons. Changes in the energy of a system are represented by movements on a multidimensional surface[33]. This surface is called the potential energy surface. For the simplest molecule it can be two-dimensional curve. With using of Cartesian coordinates the potential energy surface is 3N-dimensional, whereas with using internal coordinates it is (3N – 6)-dimensional.

The most important points on the potential energy surface are stationary points, where the first derivative of the energy is zero. At this point the forces on all the atoms are zero. One type of stationary points is minimum point, which corresponds to stable structures. A minimum can be local, global or saddle point (Fig. 16). Local minimum is the lowest point in some limited region of the potential energy surface, whereas global minimum is the lowest point anywhere on the potential surface. Global minimum representatives the most stable conformation or structural isomer, on the other hand local minimum representatives less stable conformations or structural isomers. The saddle point is maximum in one direction and minimum in the other. This point corresponds to a transition structure connecting with two equilibrium structures[34].

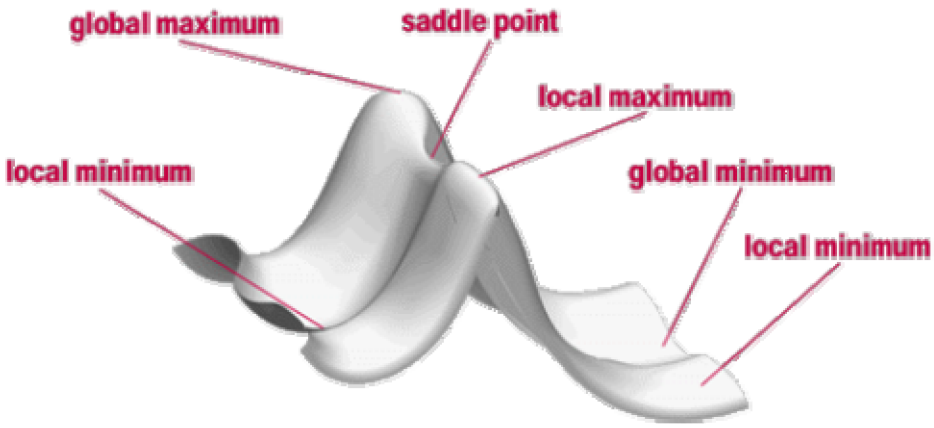

Fig. 16 The potential energy surface

2.7 Quantum mechanics

We can divide approach of quantum chemistry into semi-empirical approach, *ab initio* approach and density functional theory (DFT). Each approach will be discussed in detail in following Sections. In some older publications DFT is classified into *ab initio* methods, because both methods are similar. However DFT (will be discussed in Section 2.7.10) includes electron correlation in addition, therefore in this work this method is classified into quantum chemistry approach.

2.7.1 Atomic units

Because properties of atomic particles as electrons, protons and neutrons are expressed too small values, we work with atomic units, which simplify calculations. Relations between the atomic units and SI units (International System of Units) are in Tab. 2.

Tab. 2 Relantions between the atomis unit and SI unit

Physical quantity	Atomic units	SI units
Charge	1	$\|e\| = 1.60219 \cdot 10^{-19}$ C
Length	1	$a_0 = 5.29177 \cdot 10^{-11}$ m (1 Bohr)
Mass	1	$m_e = 9.10593 \cdot 10^{-31}$ kg
Energy	1	$E_a = 4.35981 \cdot 10^{-18}$ J (1 Hartree)

Other important relations between units[34] are: 1 Å (Ångström) = 10^{-10} m, 1 Hartree = 27.2116 eV = 2627.34 kJ·mol^{-1} = 627.5095 kcal·mol^{-1}, 1 kcal = 4.1869 kJ. In atomic units Plank's constant is $h = 2\pi$ and $\hbar = 1$.

2.7.2 Schrödinger equation

In quantum mechanics Schrödinger equation plays important role. This equation takes many different forms, depending on the physical situation. The full, time-dependent form is:

$$\left\{-\frac{\hbar^2}{2m}\left(\frac{\partial^2}{\partial x^2}+\frac{\partial^2}{\partial y^2}+\frac{\partial^2}{\partial z^2}\right)+\hat{V}\right\}\Psi(\mathrm{r},t)=i\hbar\frac{\partial\Psi(\mathrm{r},t)}{\partial t} \qquad (2.7\text{-}1)$$

where $\hbar$ is Planck's constant divided by 2π, i is imaginary unit, Ψ is wavefunction, m is the mass of particle, **r** is given by a position vector **r** = x**i** + y**j** + z**k** and time (t) under influence of an external field V (which might be the electrostatic potential because of the nuclei of a molecule).

When the external potential V is time-independent, we can write Schrödinger equation in the time-independent form:

$$\left\{-\frac{\hbar^2}{2m}\nabla^2 + \hat{V}\right\}\Psi(\mathrm{r}) = E\Psi(\mathrm{r}) \tag{2.7-2}$$

where E is the energy of particle and ∇^2 is the Laplace operator, which simplifies the equation:

$$\nabla^2 = \frac{\partial^2}{\partial x^2} + \frac{\partial^2}{\partial y^2} + \frac{\partial^2}{\partial z^2} \tag{2.7-3}$$

We can use Hamiltonian operator $\hat{H}$ to abbreviate left-hand side of the Schrödinger equation:

$$\hat{H} = -\frac{\hbar^2}{2m}\nabla^2 + \hat{V} \tag{2.7-4}$$

We get well known form:

$$\hat{H}\Psi = E\Psi \tag{2.7-5}$$

This equation says that, when the wavefunction is operated upon Hamiltonian, it is returns the wavefunction multiplied by the energy. The Schrödinger equation belongs to the category of partial differential eigenvalue equations in which an operator acts on a function (the eigenfunction) and returns the function multiplied by a scalar (the eigenvalue). The simply example of an eigenvalue equation is:

$$\frac{d}{dx}(y) = ry \tag{2.7-6}$$

This equation is first-order differential equation, where the operator is d/dx. One eigenfunction is $y = e^{ax}$ and eigenvalue is $r = a$. The Schrödinger equation is a second-order differential equation because it includes the second derivative of Ψ. A simple example of an equation is:

$$\frac{d^2y}{dx^2} = ry \tag{2.7-7}$$

The solution of this equation is:

$$y = A\cos kx + B\sin kx \tag{2.7-8}$$

where A, B and k are constant. Ψ is the eigenfunction and E the eigenvalue in the Schrödinger equation[33].

2.7.3 Operators

In quantum mechanics operators play important role. In mathematics, an operator is a mapping, which some function f(x,y) assigns function g(x,y). We will denote operators as $\hat{H}$. When we need to know the *expectation value* (average value) of a quantity such as the energy or linear momentum, we can use appropriate operator. Hamiltonian is the most commonly used operator. The energy can be determined by calculating the following integral:

$$E = \frac{\int \Psi^* \hat{H} \Psi \, dr}{\int \Psi^* \Psi \, dr} \tag{2.7-9}$$

The integral are performer over all space. Ψ^* is the complex conjugate notation, which means, that the wavefunction may be a complex number. The denominator equals 1, if the wavefunction is normalised[33].

The Hamiltonian operator consists of two parts – kinetic and potential energy. Kinetic energy operator is:

$$-\frac{\hbar^2}{2m}\nabla^2 \tag{2.7-10}$$

and the operator for potential energy includes multiplication by the appropriate potential energy. For a single electron and a single nucleus with Z protons the potential energy operator is:

$$\hat{V} = -\frac{Ze^2}{4\pi\varepsilon_0 r} \tag{2.7-11}$$

The Schrödinger equation can be solved exactly for only a few problems such as hydrogen atom or particle in a box. It is necessary to certain requirements on possible solutions to the equation. One of requirement on solution is that the wavefunction at a point r, when is multiplied by its complex conjugate, is the probability of finding particle at point. The square of an electronic wavefunction gives the electron density. The following equation must hold:

$$\int \Psi^* \Psi \, dr = 1 \tag{2.7-12}$$

Wavefunctions which satisfy this condition are normalised. Other requirement on solutions to the Schrödinger equation is to be orthogonal:

$$\int \Psi_m^* \Psi_n \, dr = 0 \quad (m \neq n) \tag{2.7-13}$$

We can express both the orthogonality of different wavefunction and the normalisation conditions using the Kronecker delta:

$$\int \Psi_m^* \Psi_n \, dr = \delta_{mn} \tag{2.7-14}$$

The Kronecker delta[33] is 1, if *m* equal *n*, whereas the Kronecker delta is 0, if m ≠ n.

2.7.4 One-electron atoms

The potential energy in one-electron atoms depends upon the distance between electron and the nucleus as given by the Coulomb equation. We can write the Hamiltonian operator in the following form:

$$\hat{H} = -\frac{\hbar^2}{2m}\nabla^2 - \frac{Ze^2}{4\pi\varepsilon_0 r} \tag{2.7-15}$$

If we use atomic unit, we get this form:

$$\hat{H} = -\frac{1}{2}\nabla^2 - \frac{Z}{r} \tag{2.7-16}$$

Z is the nuclear charge, *r* is the distance of the electron from the nucleus. One-electron atom can be hydrogen atom or helium cation. We can transform the Schrödinger equation to polar coordinates *r*, θ and ϕ, because atoms have spherical symmetry. The relationship between spherical polar and Cartesian coordinates is in Fig. 17.

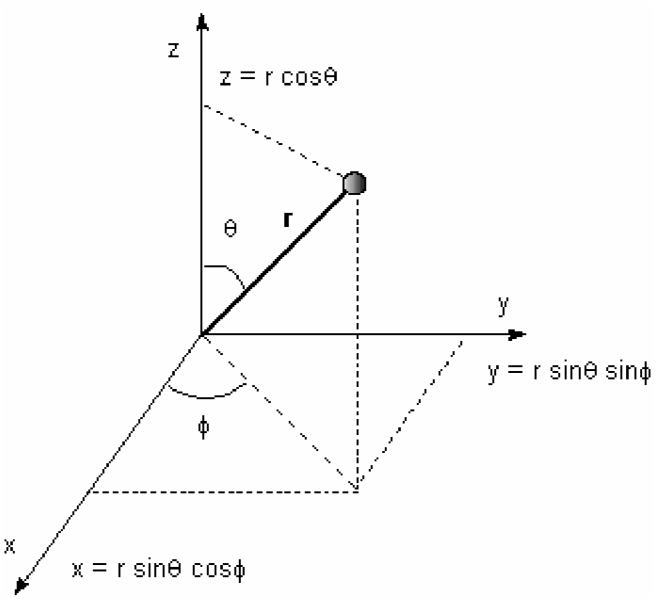

Fig. 17 The relationship between spherical polar and Cartesian coordinates

The Schrödinger equation takes form:

$$\Psi_{nlm} = R_{nl}(r)Y_{lm}(\theta,\phi) \tag{2.7-17}$$

R(r) is radial function which depends only on *r*, an angular function *Y(θ,ϕ)* called a *spherical harmonic* depends on θ and ϕ. The wavefunctions are commonly referred to as *orbitals*. Three quantum numbers *n*, *m* and *l* characterize the orbitals. These numbers can adopt following values:

1. *n*: principal quantum number: 0, 1, 2, ..., the alternative notation: K, L, M, ...
2. *l*: azimuthal quantum number: 0, 1...(n-1), the alternative notation: s, p, d, f, ...
3. *m*: magnetic quantum number: $-l$, $-(l-1)$, ... 0 ... $(l-1)$, l.

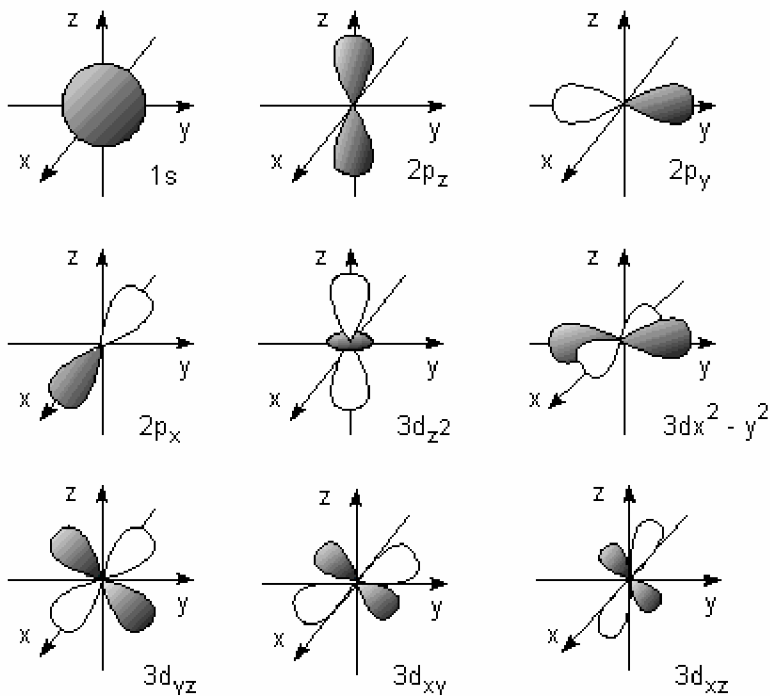

Fig. 18 The common orbitals

These orbitals are sometimes called hydrogen-like orbitals. The quantum numbers relate to the energy. Orbitals with higher quantum numbers have higher energy. Orbitals with the same value of principal quantum number but different azimuthal quantum number and magnetic quantum number are degenerate[33]. Examples of orbitals are given in Fig. 18.

2.7.5 Polyelectronic atoms and molecules

Many factors complicate the solution of the Schrödinger equation for atoms with more than one electron. For systems that include more interacting particles we can find no exact solution. Any solutions can only be approximations to the real. The principal problem is that the wavefunction is allowed to adopt more than one functional form.

In polyelectronic systems we must establish an electron spin. The spin relates to spin angular momentum and it can be described by the quantum number m_s, which for an electron takes only the value +½ and –½. Into the solution of the Schrödinger equation electron spin is incorporated. Each one-electron wave function is written as product of a spatial function and a spin function. A spatial orbital ψ (spatial part) is a function of the position vector **r** and describes the spatial distribution of an electron such that $|\psi_i(\mathrm{r})|^2 d\mathrm{r}$ is the probability of finding the electron in small volume element $d\mathbf{r}$ surrounding **r**. The spin part describes the electron spin and is marked as α or β. The wave function for an electron which describes both its spatial distribution and its spin is called a *spin orbital* χ. Two electrons with paired spin can be accommodated by each spatial orbital[35]. Electrons in polyelectronic systems occupy orbitals according to three rules:

1. The Aufbau principle – electrons fill orbitals starting at the lowest available (possible) energy states before filling higher states
2. Pauli exclusion principle – two electrons cannot share the same set of quantum numbers within the same system
3. Hund's rules – electrons occupy degenerate states with a maximum number of unpaired electrons

How it was said the Schrödinger equation can not be solved exactly for any molecular systems. When we establish the Born-Oppenheimer approximation, we can solve exactly the equation for the simplest molecular systems. This approximation assumes that the motion of the electrons is separated from the motion of the nuclei, because the masses of the nuclei are circa 1800 times heavier than masses of the electron and they move slower. Therefore the nuclei are not influenced by the motion of electrons and they are considered to be fixed. The nuclear energy is the electrostatical repulsion between nuclei and the electronic energy consists of the kinetic and potential energy of the electrons moving in the eletrostatic field of nuclei. So the total energy includes the sum of the nuclear energy and the electronic energy:

$$E_{tot} = E(\text{electrons}) + E(\text{nuclei}) \qquad (2.7\text{-}18)$$

Using of the Born-Oppenheimer approximation the Schrödinger equation is solved for the electrons alone in the field of the nuclei[33].

First formulation of the wavefunction for a polyelectronic system is known as a *Hartree product*. This formulation has a following form:

$$\Psi(1,2,\ldots \mathrm{N}) = \chi_1(1)\chi_2(2)\ldots\chi_N(\mathrm{N}) \qquad (2.7\text{-}19)$$

This form does not fulfil the antisymmetry principle, because exchanging pairs of electrons does not give the negative of the wavefunction. We can use a determinant to satisfy the

antisymmetry principle. This determinant is called Slater determinant and is the simplest form of an orbital wavefunction:

$$\Psi = \frac{1}{\sqrt{N!}} \begin{vmatrix} \chi_1(1) & \chi_2(1) & \dots & \chi_N(1) \\ \chi_1(2) & \chi_2(2) & \dots & \chi_N(2) \\ \vdots & \vdots & & \vdots \\ \chi_1(N) & \chi_2(N) & \dots & \chi_N(N) \end{vmatrix} \tag{2.7-20}$$

If we exchange any two rows of a determinant (it corresponds to exchanging two electrons), the sign of the determinant changes. If any two rows are same, the determinant vanishes[1,33].

The total energy of polyelectronic system involves three types of interactions. First energy creates the kinetic and potential energy of each electron moving in the field of the nuclei. This energy is written as H_{ii}^{core}. The contribution to the total energy for N electrons in N molecular orbitals is:

$$E_{total}^{core} = \sum_{i=1}^{N} \int d\tau_1 \chi_1(1) \left(-\frac{1}{2}\nabla_i^2 - \sum_{A=1}^{M} \frac{Z_A}{r_{1A}} \right) \chi_i(1) = \sum_{i=1}^{N} H_{ii}^{core} \tag{2.7-21}$$

Second contribution to the total energy represents Coulomb interaction between electrons in spin orbitals *i* and *j*. This interaction is represented by the symbol J_{ij} and depends on the electrons distance. The total Coulomb contribution is given by:

$$E_{total}^{Coulomb} = \sum_{i=1}^{N} \sum_{j=i+1}^{N} \int d\tau_1 d\tau_2 \chi_i(1) \chi_i(1) \frac{1}{r_{12}} \chi_j(2) \chi_j(2) = \sum_{i=1}^{N} \sum_{j=i+1}^{N} J_{ij} \tag{2.7-22}$$

The third interaction presents the exchange interaction. It is created because the motion of electrons with parallel spins is correlated. If two electrons occupy the same space and have parallel spins, they are considered to have the same set of quantum numbers. Thus electrons with the same spins tend to keep away each other. The energy because of exchange has a symbol K_{ij}. The total exchange energy is:

$$E_{total}^{exchange} = \sum_{i=1}^{N} \sum_{j'=i+1}^{N} \iint d\tau_1 d\tau_2 \chi_i(1) \chi_j(2) \left(\frac{1}{r_{12}} \right) \chi_i(2) \chi_j(1) = \sum_{j=1}^{N} \sum_{j'=i+1}^{N} K_{ij} \tag{2.7-23}$$

The spins of the electrons in the spin orbitals χ_i and χ_j are the same, if the integral is only non-zero[33].

If we calculate the energy from approximation to the true wavefunction, we always get greater energy than the true energy. So the best wavefuntion has the minimal energy. The other approximation was established by Fock. The major problem for the solution of the Schrödinger equation is the presence of interactions between the electrons. These interactions can be expressed as Coulomb and exchange integrals. Fock supposed that each electron moves in a fixed field including the nuclei and the other electrons. The *Hatree-Fock equations* express a single electron in the spin orbital χ_i in the field of the nuclei and the other electrons in their fixed spin orbital χ_i. These equations take a following form:

$$\left[-\frac{1}{2}\nabla_i^2-\sum_{A=1}^{M}\frac{Z_A}{r_{1A}}\right]\chi_i(1)+\sum_{j\neq i}\left[\int d\tau_2\chi_j(2)\chi_j(2)\frac{1}{r_{12}}\right]\chi_i(1)$$
$$-\sum_{j\neq i}\left[\int d\tau_2\chi_j(2)\chi_i(2)\frac{1}{r_{12}}\right]\chi_i(1)=\sum_j\varepsilon_{ij}\chi_j(1) \qquad (2.7\text{-}24)$$

or a simply form:

$$\hat{f}_i\chi_i=\varepsilon_i\chi_i \qquad (2.7\text{-}25)$$

$\hat{f}_i$ is the *Fock operator*, which includes three operators – the core Hamiltonian operator $\hat{H}^{core}$, the Coulomb operator $\hat{J}_j$, which corresponds to the average potential because of an electron in χ_j, and exchange operator $\hat{K}_j$. Therefore the Fock operator for a close-shell system takes this form:

$$\hat{f}_i(1)=\hat{H}^{core}(1)+\sum_{j=1}^{N/2}\left\{2\hat{J}_j(1)-\hat{K}_j(1)\right\} \qquad (2.7\text{-}26)$$

We can solve this equation as follows. First, we obtain a set of test solutions χ_i to the Hartree-Fock eigenvalue equations and we calculate the Coulomb and exchange operators. Then we calculate the Hartree-Fock equations and get a second set of solutions χ_i, which we use in the next iteration. This method is called *self-consistent field* (SCF). The individual electronic solutions correspond to lower and lower total energy until results for all electrons are unchanged[33].

For solution of Hatree-Fock equations for molecules we must agree to an alternative approach. We must express the molecular orbitals. The most common way is linear combination of atomic orbitals (LCAO):

$$\psi_i=\sum_{v=1}^{K}c_{vi}\phi_v \qquad (2.7\text{-}27)$$

ψ_i is a molecular orbital, ϕ_v, c_{vi} is a coefficient and ϕ_v is the one-electron orbitals, which correspond to the atomic orbitals. The atomic orbitals are often called as *basis function*. From K basis function we can derive K molecular orbitals, but not all of these orbitals must to be occupied by electrons. The lowest energy of system is determined by using *Roothaan-Hall* equations[33], which can be written as matrix equation:

$$\mathbf{FC}=\mathbf{SCE} \qquad (2.7\text{-}28)$$

F is Fock matrix, **C** is matrix of coefficient c_{vi}, **S** is overlap matrix and **E** is a diagonal matrix whose elements are the orbital energies ε_i.

2.7.6 Basis sets

It was said that the basis sets consist of atomic orbitals, which are used to create molecular orbitals. In *ab initio* calculations the Slater type orbitals (STOs) were first used atomic orbitals. These orbitals are not particularly amenable, because it is difficult to solve three- and four-centre integrals, if the atomic orbitals are located on different atoms. So the Slater orbitals were replaced by Gaussian type orbitals (GTOs). At the first time the Gaussian functions were used by Boys[36]. The advantage of these functions is fact that the product of two Gaussians we can express as a single Gaussian, which is located along the line joining the centres of two Gaussians. Although these functions have some defects. If we replace a Slater

type orbital by a single Gaussian function, it leads to errors. Therefore a linear combination of Gaussian functions is used. Each linear combination takes the following form:

$$\phi_\mu = \sum_{i=1}^{L} d_{i\mu}\phi_i(\alpha_{i\mu}) \qquad (2.7\text{-}29)$$

L is the number of function in the expansion, $d_{i\mu}$ is the coefficient of the primitive Gaussian function ϕ_i and $\alpha_{i\mu}$ is an exponent.

Gaussian expansion has two parameters: the coefficient and the exponent. Basis sets composed of contracted Gaussian function are the most commonly used. In a contracted function the contraction coefficients and exponents are constant during the calculation[33].

A *minimal basis set* includes the minimum number of functions required to accommodate all the filled orbitals in each atom. They contain only one contraction per atomic orbital. The most common minimal basis set is STO-nG (Slater type orbital), where *n* Gaussian functions are used to represent each orbital.

A *double zeta valence* basis set (DZV) doubles the number of functions in the minimal basis set. The SCF method calculates automatically the basis set coefficients of the contracted and the diffuse functions.

Split valence basis keeps a single function for inner shells, but doubles the number of functions which are used to describe the valence electrons. Unlike the valence orbitals the core orbitals do not influence chemical properties very much. These basis sets are marked as 3-21G. It means that three Gaussians describe the core orbitals and other three Gaussians describe electrons orbitals, where the contracted part represents two Gaussians and the diffuse part represents one Gaussians. The other used split valence basis sets are 4-31G and 6-31G.

Other type of basis sets is a *basis with polarisation functions*, which have higher angular quantum number and correspond to p orbitals for hydrogen and d orbitals for the first- and second-row elements. The asterisk * at the end of a basis set denotes polarization function. 6-31G* is a 6-31G basis with polarisation functions on heavy atoms. Two asterisks ** denotes polarisation functions on hydrogen and helium atom. It can be useful for molecules where hydrogen acts as a bridging atom.

A *basis with diffuse functions* deals with anions, cations and molecules included lone pairs. This basis set is denoted using +. If the diffuse functions are contained for hydrogen as well as for heavy metals, the basis set is denoted using ++[33].

Common standard basis sets[37] are:

1. MINI - Huzinaga's 3 gaussian minimal basis set
2. MIDI - Huzinaga's 21 split valence basis set
3. STO - Pople's STO-NG minimal basis set
4. N21 - Pople's N-21G split valence basis set
5. N31 - Pople's N-31G split valence basis set
6. N311 - Pople's "triple split" N-311G basis set
7. DVZ – "double zeta valence basis set"
8. DH – Dunning/Hay "double zeta" basis set
9. TZV – "triplet zeta valence" basis set
10. MC – McLean/Chandler "triple split" basis

2.7.7 Electron correlation

The most important disadvantage of Hatree-Fock method is that it can not represent electrons correlation. In the self-consistent field method the electrons are assumed to be

moving in an average potential of the other electrons. In reality, the motions of electrons are correlated and they tend to "avoid" each other. Difference between the Hartree-Fock energy and the exact energy is called the correlation energy. If the electron correlation is neglected, we can get some clearly anomalous results. The inclusion of correlation effect is warranted, although Hatree-Fock geometries are often in good agreement with experiment. Electron correlation is essential in the study of dispersive effects. It is often discussed in *ab initio* methods, but effects of electron correlation are involving in the semi-empirical methods[33].

2.7.8 Using *ab initio* methods

In the *ab initio* methods we do use no empirical data in their calculations. The term *ab initio* means that the calculation is from first principles. This method is based on the laws of quantum mechanics and on the values of a small number of physical constants:

1. The masses and charges of electrons and nuclei
2. The speed of light
3. Planck's constant

The *ab initio* calculation offers high quality quantitative predictions for many systems, however it can take on the order of one to a few days, therefore it is often expansive. It is usually used for several tens of atoms[34]. The most popular *ab initio* methods we can divide into three main classes: the Hatree-Fock methods, post-Hartree-Fock methods and multi-reference methods. In post-Hartree-Fock methods correlation effects are incorporated, the most popular approaches are Configuration interaction (CI), Quadratic Configuration Interaction (QCI), Møller-Plesset Pertubation Theory (MP2, MP3 or MP4) or Coupled Cluster (CC). We classify multireference methods into Multi-configurational self-consistent field (MCSCF), Multireference single and double configuration interaction (MRDCI) and N-elecron valence state pertubation theory (NEVPT). For our calculations we will use only Hartree-Fock methods, which include Restricted Hartree Fock (RHF), Unrestricted Hartree Fock (UHF) and Restricted open shell Hartree Fock (ROHF) calculation. RHF is the most used method.

We can use this method for the simple single point calculation as well as for geometry optimization, frequency calculation, electric multipoles, total electron density distribution and molecular orbitals or thermodynamic properties. The most common calculation but the most exacting is geometry optimization, which is an important step for frequency calculation.

The electric multipoles express the distribution of charge in a molecule. The simplest example of electric moment is the dipole, which is a vector quantity, with components along the three Cartesian axes.

The electron density can be calculated from Born interpretation of the wavefunction as a sum of squares of the spin orbital for all molecular orbital:

$$\rho(\mathrm{r}) = 2\sum_{i=1}^{N/2} |\psi_i(\mathrm{r})|^2 \qquad (2.7\text{-}30)$$

We can visualise the electron density as a solid object, whose surface connects points of equal density. On this surface we can map the electrostatic potential or other properties. Using the electron density distribution of individual molecular orbitals we can determine and plot HOMO and LUMO, which influence reactivity of molecules. We can order molecular orbitals from highest energy to lowest energy:

1. σ* - almost never occupied in the ground state
2. π* - very rarely occupied in the ground state
3. n - nonbonding (lone pairs)
4. π - always occupied in compounds with multiple bonds (π bond)
5. σ - at least one occupied in all molecules (σ bond)
6. a - an empty orbital

The electrostatic potential is defined as the work done to bring unit positive charge from infinity to the point and it has contributions from both the nuclei and from the electrons. It is responsible for interactions between molecules and it can determine where electrophilic attack can occur. Electrophiles are attracted to regions with negative electrostatic potential[33].

2.7.9 Semi-empirical methods

Semi-empirical methods use parameters derived from experimental data. They solve an approximate form of the Schrödinger equations. Unlike *ab initio* method they are relative inexpensive and we can calculate very large molecules. The most popular semi-empirical methods are AM1, PM3 and MNDO. We can first calculate semi-empirical optimization to obtain a starting structure for Hatree-Fock or Density Functional Theory optimization. These methods can quickly calculate molecular orbitals or vibrational normal modes. However they have some problems with systems including hydrogen bonding, transitional structures and with molecules containing atoms for which they are poor parametrized[34].

2.7.10 Density functional theory

Density functional theory methods are similar to *ab initio* methods and they are generally less expensive. The best DFT methods achieve greater accuracy than Hartree-Fock methods and they increase modest the cost. These methods contain the effects of electron correlation, which is calculated via general functionals of the electron density. DFT functionals distribute the electronic energy into numbers of components which are computed separatly: the kinetic energy, the electron-nuclear interaction, the Coulomb repulsion and an exchange-correlation term accounting for the remainder of the electron-electron interaction. We can divide funtionals in two groups: traditional and hybrid functional. The traditional functionals treat the exchange and correlation components - *local* exchange and correlation functionals, which include the value of the electron spin densities and *gradient-corrected* functionals include value of electron spin densities and their gradients. The hybrid functionals define the exchange functional as a linear combination of Hartree-Fock and gradient-corrected exchange terms[34].

2.8 Molecular mechanics

Molecular mechanics uses Newtonian mechanics to predict the structures and properties of molecules. The potential energy of all systems is calculated using force fields, which include these components:

1. A set of equation describing variation of the potential energy of a molecule with the location of its component atoms
2. A series of atoms describing characteristics of an element
3. One or more parameter sets that fit the equations and atom types to experimental data

Bonded interactions are treated as “springs” with an equilibrium distance equal to the experimental or calculated bond length .

These calculations do not explicity treat the electrons in a molecular system, so they perform computitation based upon the interactions among the nuclei. Electronic effects are implicitly involved in force fields though parametrization.

This approximation makes molecular mechanics calculations quite inexpensive computionally, and allows them to be used for very large systens including many thousands of atoms. Although, it carries several limitations as well[34].

2.9 Geometry optimization

For geometry optimization an isolated molecule in vacuum is usually taken. The finding of the conformation with the lowest energy is main point of geometry optimization. We use a *minimalisation algorithm* to identify geometries of the system that correspond to minimum points on the energy surface. Using of geometry optimization we can search too the saddle points, which correspond to the transition structure. The ideal minimisation algorithm provides the answer as quickly as possible, using the least amount of memory. Most software packages offer a choice of methods. For quantum mechanics other methods are used than for molecular mechanics. Most minimisation algorithms can only go downhill on the energy surface; therefore they can only locate the nearest minimum to the starting point. To locate the global energy minimum we must generate different starting points, each point is then minimised[33].

To distinguish between minima, maxima and saddle point we must calculate the eigenvalues of the Hessian matrix, which is the square matrix of second-order partial derivatives of a function. At a minimum point there must be the six zero and $3N$ (for Cartesian coordinates) positive eigenvalues. The six zero eigenvalues correspond to the transitional and rotational degrees of freedom of the molecule. At a maximum point all eigenvalues must be negative and at a saddle point must be one or more eigenvalues negative. In real molecular modelling applications it is impossible to find exact location of minima or saddle points. Therefore we find an approximation of these points. We monitor the energy from one iteration to the next and stop when the difference in energy between successive steps falls below a specified threshold. This specified threshold is called convergence criteria. A second method is to monitor the change in coordinates and a third method is to calculate the root-mean-square gradient:

$$RMS = \sqrt{\frac{g^T g}{3N}} \tag{2.9-1}$$

We can distinguish two groups of minimisation algorithms: those which use derivatives of the energy with respect to the coordinates and those which do not[33].

2.9.1 Non-derivative minimisation methods

Non-derivative minimisation methods use the simplex method or the sequential univariate method. The simplex method is expensive in terms of computer time because of the large number of required energy evaluations. Therefore this method is used in combination with a

different minimisation algorithm. For quantum mechanical calculation the sequential univariate method is more suitable than the simplex method. It usually requires fewer function evaluations but it can be slow to converge[33].

2.9.2 Derivative minimisation methods

Derivatives provide information about the shape of the energy surface, therefore they can improve the efficiency with the minimum is located. The direction of the first derivative of the energy (gradient) indicates where minimum lies, and magnitude of the gradient indicates the steepness of the local slope. Second derivatives show the curvature of the function, information that can be used to predict where the function will change direction (i.e. pass through a minimum or some other stationary point). We can classify the derivative methods according to the highest-order derivative used. While first-order methods use first derivatives, second-order methods use both first and second derivatives.

Unlike analytical first derivatives analytical second derivatives are only available for a few levels of quantum mechanics theory and can be expensive in terms of computer time[33].

2.10 Infrared and Raman spectroscopy

How it was written in Section 2.7.5, the total energy consists of the sum of the nuclear energy and the electronic energy. However we fell into an error, because we do not include the vibrations of a molecule. If the molecule absorbs energy, the electronic, the rotational and vibrational states can change. A transfer of energy will occur, when Bohr's frequency condition is satisfied:

$$\Delta E = E_2 - E_1 = h\nu \tag{2.10-1}$$

The transition is allowed, if the selection rules are valid. Electronic transitions mainly occur in the 10^4-10^6 cm^{-1} region UV-visible region), because their level are wide apart, rotational transitions principally appear in the 1-10^2 cm^{-1} region (microwave region) because rotational levels are relatively close to each other, whereas vibrational transitions appear in the 10^2-10^4 cm^{-1} region and originate from vibrations of nuclei. In IR (Infrared) and RA (Raman) spectra vibrational and rotational states change, however the rotational transitions have a little signification and they can be measured mainly in the gaseous state. Below each electronic level there is "zero-point energy" which must exist even at a temperature of absolute zero as a result of Heisenberg's uncertainty principle:

$$E_0 = \frac{1}{2}h\nu \tag{2.10-2}$$

In the Born-Oppenheimer and harmonic oscillator approximations the resonance frequencies are determined by the normal modes corresponding to the molecular electronic ground state potential energy surface[38].

2.10.1 Vibrations of diatomic molecule

Using of the quantum mechanics, the vibration of two nuclei in a diatomic molecule can be reduced to the motion of a single particle of mass μ, whose displacement q from its

equilibrium position is equal to the change of the internuclear distances. The mass μ is called the reduced mass and is given by:

$$\frac{1}{\mu} = \frac{1}{m_1} + \frac{1}{m_2} \tag{2.10-3}$$

For the system representing a harmonic oscillator the kinetic energy takes form:

$$T = \frac{1}{2}\mu\dot{q}^2 = \frac{1}{2\mu}p^2 \tag{2.10-4}$$

where p is conjugate momentum $\mu\dot{q}$.

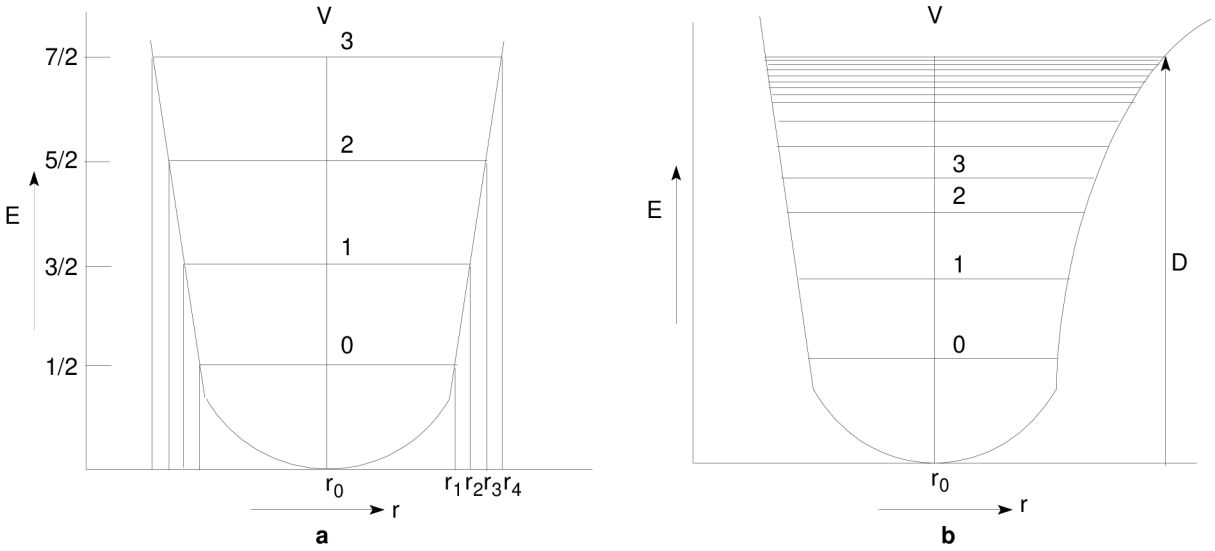

Fig. 19 The potential curves

For a harmonic oscillator a potential curve is parabolic (Fig. 19a), therefore we can define potential energy as:

$$V = \frac{1}{2}Kq^2 \tag{2.10-5}$$

where K is the force constant for the vibration. From Schrödinger equation we can get eigenvalues:

$$E_v = hv\left(\upsilon + \frac{1}{2}\right) \tag{2.10-6}$$

where υ is the vibrational quantum number and v is frequency of vibration that is given by:

$$v = \frac{1}{2\pi}\sqrt{\frac{K}{\mu}} \tag{2.10-7}$$

Then we can express the wavenumber as:

$$\tilde{v} = \frac{1}{2\pi c}\sqrt{\frac{K}{\mu}} \tag{2.10-8}$$

In conclusion frequency of vibration depends on force constant and reduced mass. However the actual potential curve differs (Fig. 19b), therefore the wavenumber of normal vibration is corrected for anharmonicity ω_e. Then the eigenvalues are given as:

$$E_v = hc\omega_e\left(\upsilon+\frac{1}{2}\right) - hcx_e\omega_e\left(\upsilon+\frac{1}{2}\right)^2 + \ldots \tag{2.10-9}$$

where $x_e\omega_e$. indicates the magnitude of anharmonicity. The anharmonicity is responsible for the occurrence of overstones and combination vibrations, which are forbidden in the harmonic oscillator. Then the force constant for anharmonicity can be expressed:

$$K = 4\pi^2 c^2 \omega_e^2 \mu \tag{2.10-10}$$

The force constant determines the bond strength in this case and can be calculated by quantum mechanicals methods as well as by the determination from the analysis of vibrational spectra[38].

2.10.2 Polyatomic molecules

In polyatomic molecules the situation is more complicated because all nuclei perform their own harmonic oscillators. Extremely complicated vibrations of the molecule can be represented as a superposition of a number of normal vibrations. The kinetic energy depends on the masses of the individual atoms and their geometrical arrangement in the molecule:

$$T = \frac{1}{2}\sum_{i}^{3N}\dot{q}_i^2 \tag{2.10-11}$$

On the other hand the potential is determined interaction between the individual atoms and is described in terms of the force constant that can be obtained from the observed frequencies:

$$V = \frac{1}{2}\sum_{ij}^{3N}\left(\frac{\partial^2 V}{\partial q_i \partial q_j}\right)_0 q_i q_j = \frac{1}{2}\sum_{ij}^{3N} b_{ij} q_i q_j \tag{2.10-12}$$

For the equilibrium we can solve following equation:

$$\ddot{q}_i + \sum_j b_{ij} q_j = 0 \tag{2.10-13}$$

Then for the equilibrium position this equation holds:

$$q_i = q_i^0 \sin\left(\sqrt{b_{ii}}t + \delta_i\right) \tag{2.10-14}$$

where q_i^0 is the amplitude and δ_i is the phase constant. The coordinates q_i must be transformed into a set of new coordinates Q_i according to the relations:

$$q_1 = \sum_i B_{1i} Q_i \tag{2.10-15}$$

The Q_i are called normal coordinates and the equation (2.10-13) takes following form:

$$Q_i = Q_i^0 \sin\left(\sqrt{\lambda_i}t + \delta_i\right) \tag{2.10-16}$$

Then the frequency can be expressed as:

$$\nu_i = \frac{1}{2\pi}\sqrt{\lambda_i} \tag{2.10-17}$$

where ν_i is called a normal vibration[38].

Nonlinear molecules have 3N-6 degrees of vibrational modes (called vibrational degrees of freedom), because six coordinates are required to describe the translational and rotational motion of the molecule as a whole. On the other hand linear molecules have 3N-5 degrees of vibrational modes, because no rotational freedom exists around the molecular axis. The general form of molecular vibration is a superposition of the 3N-6 (or 3N-5) normal vibrations. When all the normal vibrations are independent of each other, consideration may

be limited to a special case in which only one normal vibration is excited. So in the normal vibration, all the nuclei move with the same frequency and in phase. The equation (2.10-13) can be written in the more general form:

$$q_k = A_k \, sin\left(\sqrt{\lambda}t + \delta\right) \tag{2.10-18}$$

The following equation must be solved:

$$-\lambda A_k + \sum_j b_{kj} Aj = 0 \tag{2.10-19}$$

This is a system of first-order simultaneous equations. Since all As must be nonzero, we must solve following equation:

$$\begin{vmatrix} b_{11}-\lambda & b_{12} & b_{13} & \cdots \\ b_{21} & b_{22}-\lambda & b_{23} & \cdots \\ b_{31} & b_{31} & b_{33}-\lambda & \cdots \\ \vdots & \vdots & \vdots & \end{vmatrix} = 0 \tag{2.10-20}$$

To calculate the vibrational frequencies it is useful to express potential and kinetic energies in internal coordinates R_i, which do not involve translational and rotational motion of the molecule. Using these coordinates we can express the potential energy as:

$$2V = \widetilde{R}FR \tag{2.10-21}$$

where R is a column matrix, $\widetilde{R}$ is its transpose and F (hessian) is a matrix whose component are the force constants:

$$F = \begin{bmatrix} f_{11} & f_{12} & r_1 f_{13} \\ f_{21} & f_{22} & r_2 f_{23} \\ r_1 f_{31} & r_2 f_{32} & r_1 r_2 f_{33} \end{bmatrix} \equiv \begin{bmatrix} F_{11} & F_{12} & F_{13} \\ F_{21} & F_{22} & F_{23} \\ F_{31} & F_{32} & F_{33} \end{bmatrix} \tag{2.10-22}$$

where r_1 and r_2 are the equilibrium lengths of the X-Y_1 and X-Y_2 bonds. The F matrix elements are refined until differences between the calculated and observed frequencies are minimized. The kinetic energy can be express as:

$$2T = \dot{\widetilde{\mathrm{R}}}\mathrm{G}^{-1}\dot{\mathrm{R}} \tag{2.10-23}$$

where G^{-1} is the reciprocal of the G matrix, which is defined as:

$$G = BM^{-1}\widetilde{B} \tag{2.10-24}$$

where B is matrix, M^{-1} is diagonal matrix whose components are the reciprocals of the masses of *i*th atom. The G matrix element can be calculated from the known bond distances and angles. Then we can solve the matrix secular equation:

$$\left|GF - E\lambda\right| = 0 \tag{2.10-25}$$

where E is the unit matrix. As results we obtain the wavelengths that are converted to the wavenumbers. If the order of the secular equation is higher than three, it is too difficult to solve it. Symmetry of a molecule can significantly simplify the calculations[38].

2.10.3 Principle of IR and RA spectroscopy

The principle of IR spectroscopy is absorption of infrared radiation by molecules. IR spectroscopy can be divided into three regions: near-infrared 14000-4000 cm^{-1}, mid-infrared 4000-400 cm^{-1} (most used) and far-infrared (400-10 cm^{-1}). IR radiation is electromagnetic radiation, which has longer wavelength and lowers the frequency than that of visible light. Its

energy is not enough for changes electronic ground states, but it causes changes of rotational-vibrational states of the molecule, however the vibrational transitions predominate.

Raman spectra have their origin in the electronic polarization caused by ultraviolet, visible and near-IR light. Raman spectroscopy uses the scattering of the monochromatic light (laser) and spectra are represented as shifts of the incident frequency in ultraviolet, visible and near-IR region[38]. Both IR and RA spectra can be obtained from samples in all phases (gaseous, liquid, solid).

The vibrations can be divided into two basic groups: stretching and bending vibrations. The atoms in a CH_2 group can vibrate in six different ways: stretching vibrations (symmetric and asymmetric), planar (bending) vibrations (scissoring and rocking), out of plane (bending) vibrations (wagging and twisting). The stretching vibrations appear in region 4000-1500 cm^{-1} (sometimes called the group frequency region). On the other hand bending vibrations appear in region 1500-400 cm^{-1} (called finger print region). This region involves a very complicated series of absorptions and it is more difficult to choose individuals bonds, however every organic compound produces a unique pattern in this part of the spectrum.

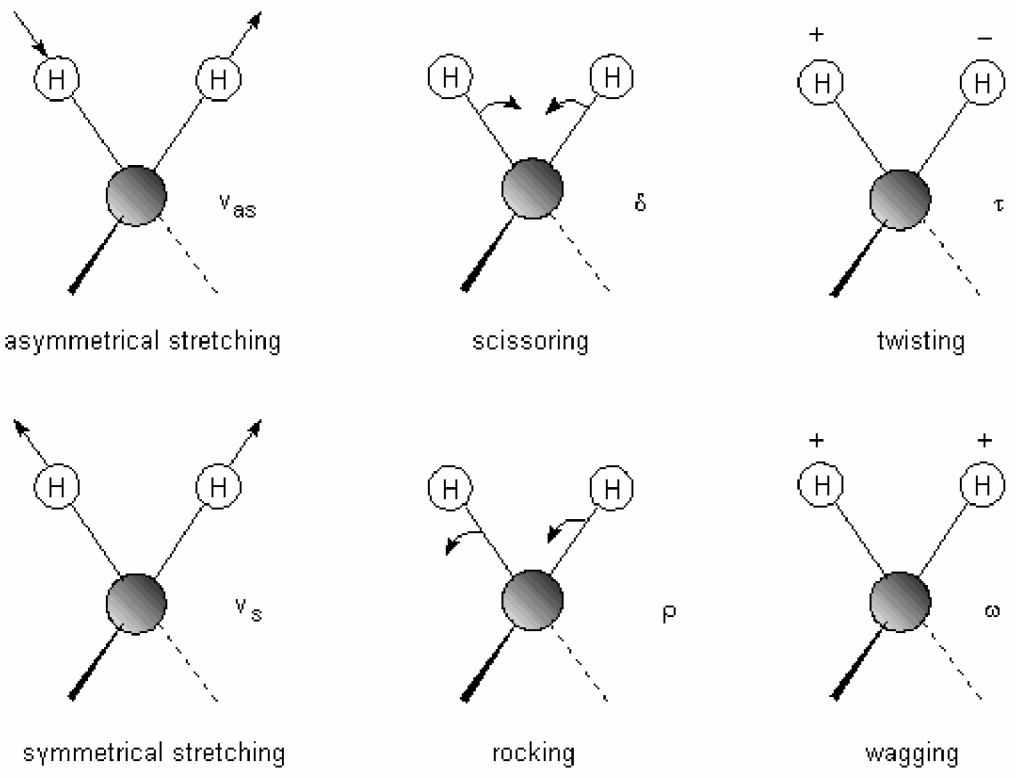

Fig. 20 Vibrations of a CH_2 group

The vibrational mode in molecule is IR active, when it is associated with changes in the dipole moment. On the other hand the vibrational mode in molecule is Raman active, when it is associated with changes in the polarization. In molecules with a centre of symmetry, asymmetrical stretching and bending will be IR active and Raman inactive, whereas symmetrical stretching and bending will be Raman active and IR inactive. For molecules without a centre of symmetry, each vibrational mode may be IR active, Raman active, both, or neither[39].

2.10.4 Prediction of spectra

Spectra are usually predicted in gaseous phase at 298.15 K. Computations use an idealized view of nuclear position. In reality, the nuclei in molecules are constantly in motion. In equilibrium states, these vibrations are regular and predictable and molecules can be identified by their characteristic spectra. Programs can compute the vibrational spectra of molecules in their ground and excited states, describe the displacements a system and predict the direction and magnitude of the nuclear displacement that occurs when a system absorbs a quantum of energy.

Molecular frequencies as well as the distinguishability between minima (discussed in Section 2.9) depend on the second derivative of the energy with respect to the nuclear positions. Programs can compute analytic second derivatives for the HF and DFT. Frequency calculations are valid only at stationary points on the potential energy surface, therefore must be done on optimized structures[34]. Computed frequencies at the Hartree-Fock level contain known systematic errors because of the neglect of electron correlation, therefore it is usual to scale frequency predicted at the HF/6-31* level by empirical factor[40] of 0.8953 and at HF/6-31+G* level by empirical factor of 0.8970. For the DFT (B3LYP)/6-31G* level is empirical factor of 0.9613.

2.11 Computer programs

A variety of computer programs are utilized to calculate the structures and properties of molecules. Among efficient ab initio computer programs belongs GAUSSIAN, PC GAMESS/Firefly, GAMESS (US), GAMESS (UK), MOLCAS or MOLPRO. Moreover they usually involve density functional theory (DFT), molecular mechanics or semi-empirical methods. We will use PC GAMESS/Firefly[41,42], which is based on GAMESS (US). GAMESS is abbreviation of General Atomic and Molecular Electronic Structure System. It can calculate single-point energies, geometry optimizations or predictions of IR and Raman intensities. It does not include a graphical user interface, therefore we used softwares for the creating of input files and for the visualization of results. For that reasons ArgusLab[43] or Gabedit[44] can be perform. Gabedit[44] can graphically display many calculation results as molecular orbitals, surfaces from the electron density, electrostatic potential or NMR shielding density and UV-Vis, IR and Raman spectra. Unlike Gabedit[44] ArgusLab[43] allows simple calculations or pre-optimizations. It can calculate and display molecular orbitals or electrostatic potential-mapped electron density surfaces.

2.11.1 The formation of input file

In ArgusLab[43] the framework of structure was built by the right-clicking the mouse button in the graphics part of the molecule window using automatic bonds function. Moreover the function for adding hydrogen CTRL+H were used. Selected atoms and bonds were mark and changed by the right-clicking the mouse button according to Fig. 21.

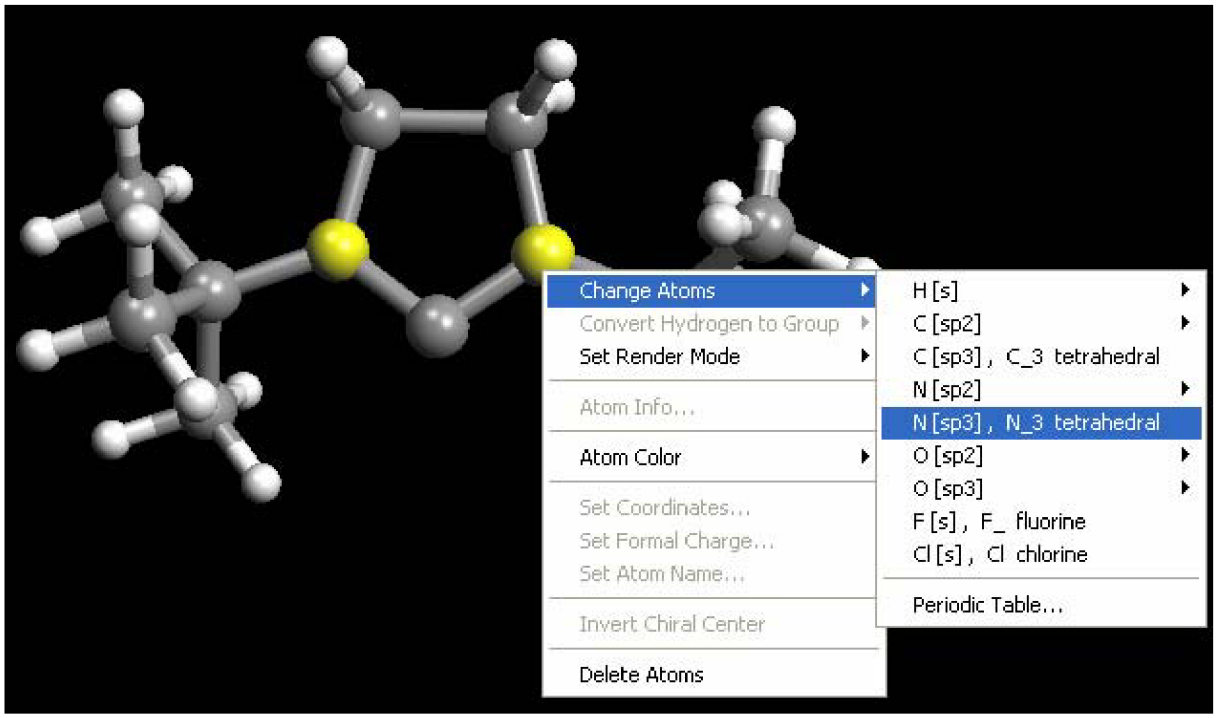

Fig. 21 The change of atoms in ArgusLab

Then the molecule was saved and the dialog box was opened in Calculation/Optimize geometry. The AM1 radio button in the Hamiltonian group box in the upper left of the dialog (Fig. 22) was chosen and the geometry optimization was run. After that the output file was viewed and optimized coordinates (Fig. 23) was found. More detailed informations are available from Tutorials and Frequently Asked Questions in AgrusLab[43].

The coordinates obtained by ArgusLab[43] were copied into notepad, where in the next step the input file for PC GAMESS/Firefly[41,42] was created.

The coordinates were set up into PC GAMESS/Firefly[41,42] format, thus the name of method, the symmetry, the name of atom and the nuclear charge was added. Then these groups were defined: $CONTRL, $SYSTEM, $SCF, $GUESS, $BASIS and $STATPT (Fig. 24) according to PC GAMESS/Firefly documentation[37].

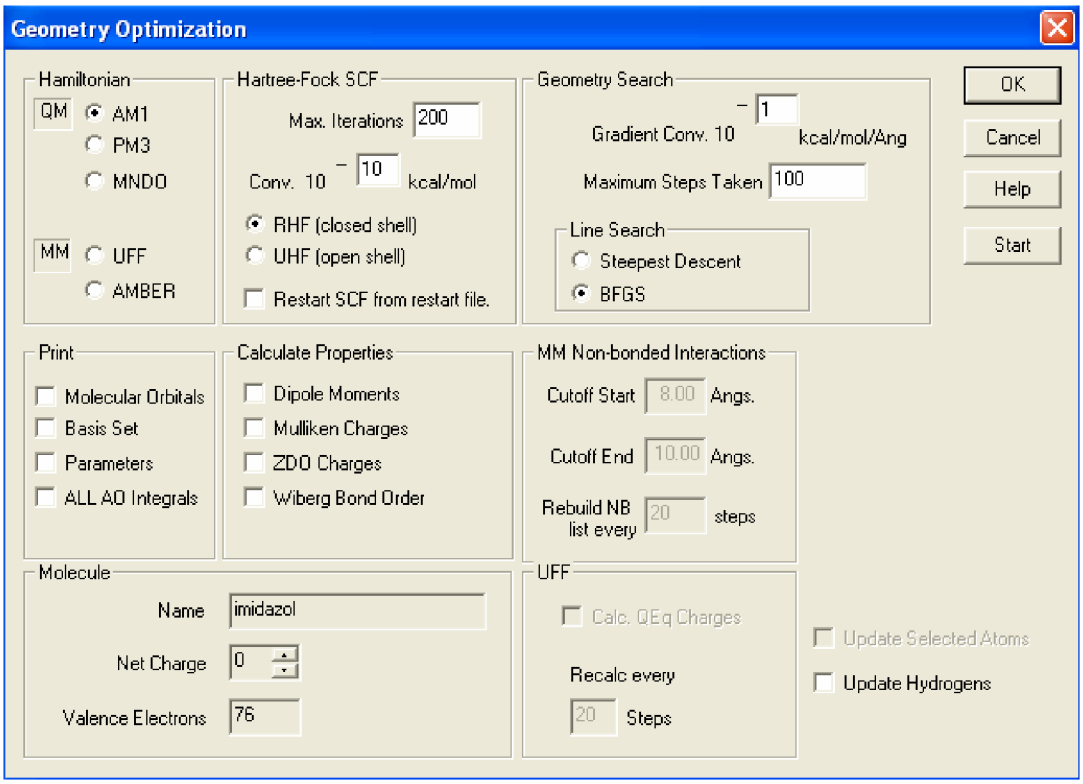

Fig. 22 The setting of geometry optimization in ArgusLab

```
******************  Final Geometry ******************

 N    29.23798792  -19.57979490   -2.11399092      7
 C    28.10814618  -20.34051731   -1.95696184      6
 N    27.01215633  -19.52433250   -2.07854187      7
 C    27.37402603  -18.12373491   -2.31701886      6
 C    28.93758699  -18.16566828   -2.36046521      6
 C    25.63620772  -19.97534445   -1.93630369      6
 C    30.59897358  -20.08907423   -2.08158694      6
 C    31.49282436  -19.24449202   -1.14938705      6
 C    30.62711735  -21.54327481   -1.57063913      6
 C    31.24156199  -20.07407230   -3.48505642      6
 C    24.64395771  -18.99274022   -2.58728215      6
 C    25.44423306  -21.35051556   -2.60903677      6
 C    25.24397294  -20.12378389   -0.45068888      6
 H    26.95095132  -17.75996273   -3.28716934      1
 H    29.38498790  -17.51676976   -1.56601841      1
 H    31.64459155  -18.22267470   -1.56821432      1
 H    32.48530419  -19.74258361   -1.05424905      1
 H    31.03875217  -19.15545957   -0.13512439      1
 H    30.02755377  -22.20358631   -2.23969738      1
 H    31.68283003  -21.89970229   -1.55156468      1
 H    30.20081286  -21.60387893   -0.54273663      1
 H    30.69090156  -20.75555511   -4.17439528      1
 H    31.23524414  -19.04611662   -3.91600458      1
 H    32.29746030  -20.42010369   -3.40231859      1
 H    23.61398570  -19.40681514   -2.48428349      1
 H    24.68109003  -17.99781937   -2.08533359      1
 H    24.86815418  -18.86084524   -3.67150261      1
 H    24.39099310  -21.68301919   -2.46298164      1
 H    26.13558555  -22.10151779   -2.15899573      1
 H    25.65485257  -21.28279053   -3.70126013      1
 H    25.34992833  -19.15368360    0.08703601      1
 H    25.89180237  -20.88278390    0.04687895      1
 H    24.18222587  -20.45565908   -0.38599161      1
 H    27.00767262  -17.46596043   -1.48907413      1
 H    29.32522487  -17.84203013   -3.35927968      1

Final Geom Energy =  -78.0544234016 au
Final Geom Energy =     -48979.9344 kcal/mol
```

Fig. 23 Example of optimized coordinates in ArgusLab

```
 $CONTRL SCFTYP=RHF  RUNTYP=OPTIMIZE MAXIT=200 $END
 $SYSTEM MWORDS=100 $END
 $SCF    DIRSCF=.True. $END
 $GUESS  GUESS=HUCKEL $END
 $BASIS  GBASIS=N31 NGAUSS=6 $END
 $STATPT NSTEP=200 $END
 $DATA
RHF/6-31G
C1
Carbon      6.0    20.638020762   -13.948361759    -1.606087026
Nitrogen    7.0    19.408631440   -13.355160586    -1.464909875
Carbon      6.0    19.519534525   -11.964651092    -1.174118263
Carbon      6.0    20.859431995   -11.684410698    -1.155787022
Nitrogen    7.0    21.524902376   -12.913079531    -1.438607639
Carbon      6.0    18.091317472   -14.078949549    -1.480948984
Carbon      6.0    17.021147065   -13.187967565    -2.131263888
Carbon      6.0    18.220579398   -15.386828354    -2.272008271
Carbon      6.0    17.679316567   -14.399516667    -0.034207518
Carbon      6.0    23.020679861   -13.063860798    -1.427627091
Carbon      6.0    23.676014047   -11.881661372    -2.158691096
Carbon      6.0    23.418399058   -14.372525734    -2.124263092
Carbon      6.0    23.509913052   -13.097371562     0.029839747
Hydrogen    1.0    18.652975776   -11.317585012    -1.024801253
Hydrogen    1.0    21.374054762   -10.740194985    -0.977138585
Hydrogen    1.0    17.229921436   -13.011116894    -3.194854812
Hydrogen    1.0    16.033503258   -13.661228692    -2.062123989
Hydrogen    1.0    16.958140737   -12.205551388    -1.636529130
Hydrogen    1.0    18.430858086   -15.200853763    -3.333471196
Hydrogen    1.0    19.034782980   -16.013320811    -1.879721762
Hydrogen    1.0    17.286438284   -15.960230590    -2.211631833
Hydrogen    1.0    16.715034497   -14.924422243    -0.015624834
Hydrogen    1.0    18.415529378   -15.047014087     0.460706013
Hydrogen    1.0    17.571791570   -13.488851374     0.570248372
Hydrogen    1.0    23.363453981   -11.827352432    -3.210004810
Hydrogen    1.0    23.431373143   -10.919008305    -1.686728975
Hydrogen    1.0    24.769028576   -11.984931459    -2.144385093
Hydrogen    1.0    23.172719118   -14.352691722    -3.194229711
Hydrogen    1.0    24.499650678   -14.538326025    -2.031667151
Hydrogen    1.0    22.899197974   -15.236060624    -1.683725786
Hydrogen    1.0    24.603748610   -13.185886796     0.065970117
Hydrogen    1.0    23.233060103   -12.184468918     0.574259822
Hydrogen    1.0    23.092549514   -13.954158664     0.575534607
 $END
```

Fig. 24 Example of the input file for PC GAMESS/Firefly

2.11.2 The formation and the manipulation with the output file

For the geometry optimization the output file was created from the input file. Program WinSCP[45] was used to transfer input files in the INP format between a local and a remote computer (server pig.ro.vutbr.cz), whereas program PuTTy[46] was used to run a calculation (Fig. 25) using the command line. The command **cd** changes directory, **dir** briefly lists directory contents, **/home2/sw/fch/PC_GAMESS_Firefly/MPICH/IntelCore2/pcgamess** describes the location of PC GAMESS/Firefly[41,42], **-i /home/zidek/kulovana/np/pre2.inp** specifies of input file to use, **-t /home/zidek/kulovana/np** creates temporary working directories to store all intermediate working files, **-o /home/zidek/kulovana/np/pre2.out** specifies of output file to use, **-p /home/zidek/kulovana/np/** redirects all text output files from working directory to the directory where the main output file resides, very important command **–nompi** forces purely sequential execution avoiding any MPI calls and **exit** closes the shell. Program WinSCP[45] can serve as freeware FTP (File Transfer Protocol) and SFTP (Secure File Transfer Protocol) client, whereas program PuTTy[46] can act as a client for SSH (Secure Shell) or raw TCP (Transmission Control Protocol) computing protocol.

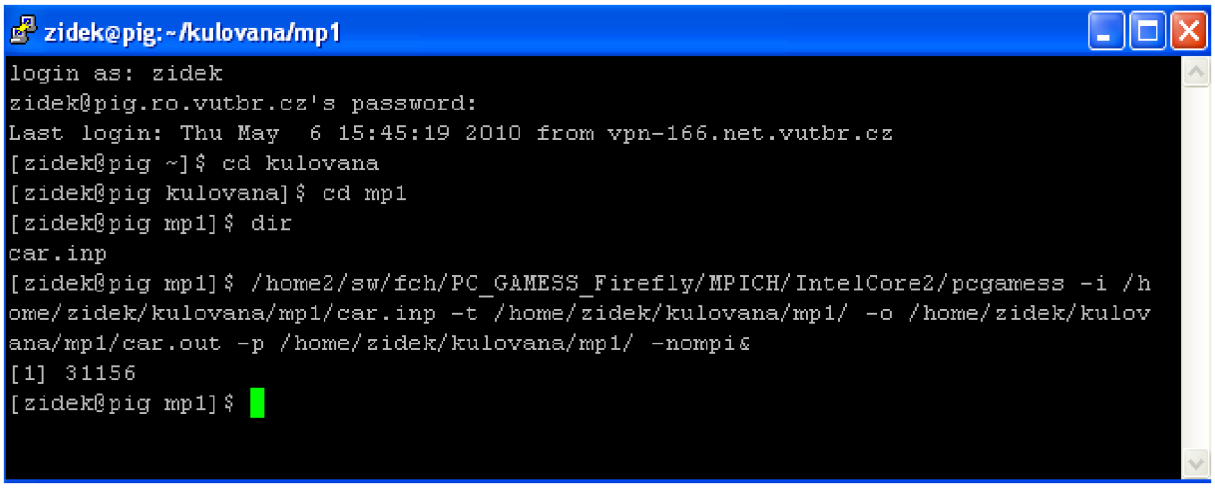

Fig. 25 The running a calculation in PuTTy

From the output file, which can be opened in the notepad, in RUNpcg[47] the ENT file was generated (Fig. 26). This file was opened in ArgusLab[43] and the selected bond distances and angles were found.

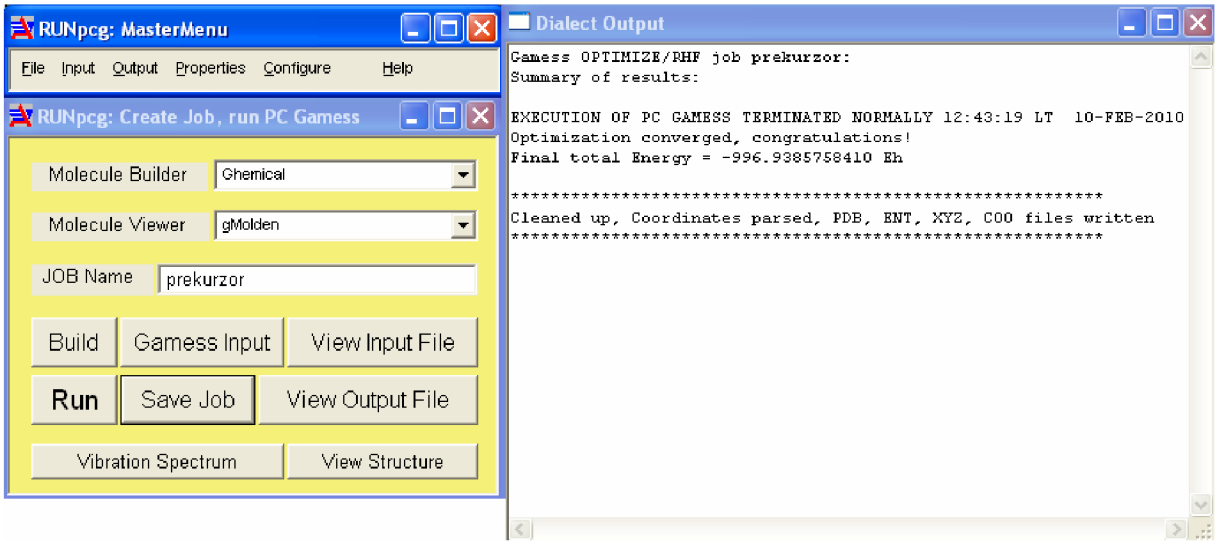

Fig. 26 Generating of ENT file

The output file for the IR and RA spectra was created from the input file by the same way as for the geometry optimization. Both spectra were read (Fig. 27), visualized (Fig. 28) and converted into XY format in Gabedit[44]. Subsequently, spectra were set up in Excel[52].

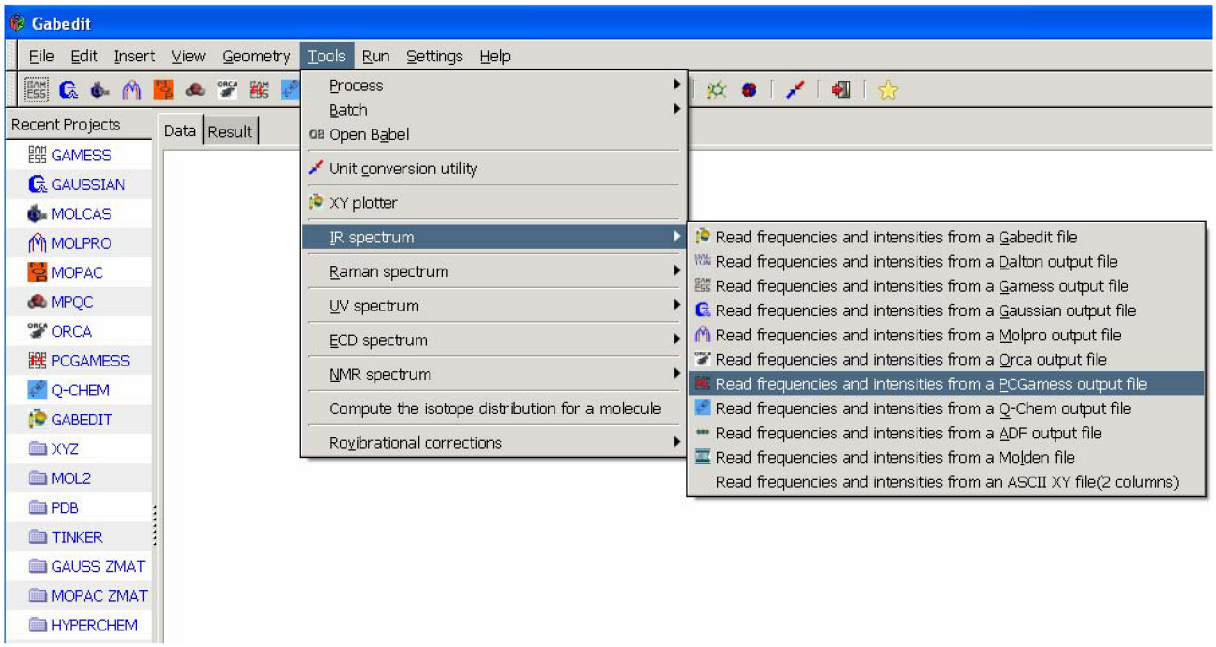

Fig. 27 Reading of IR spectrum in Gabedit

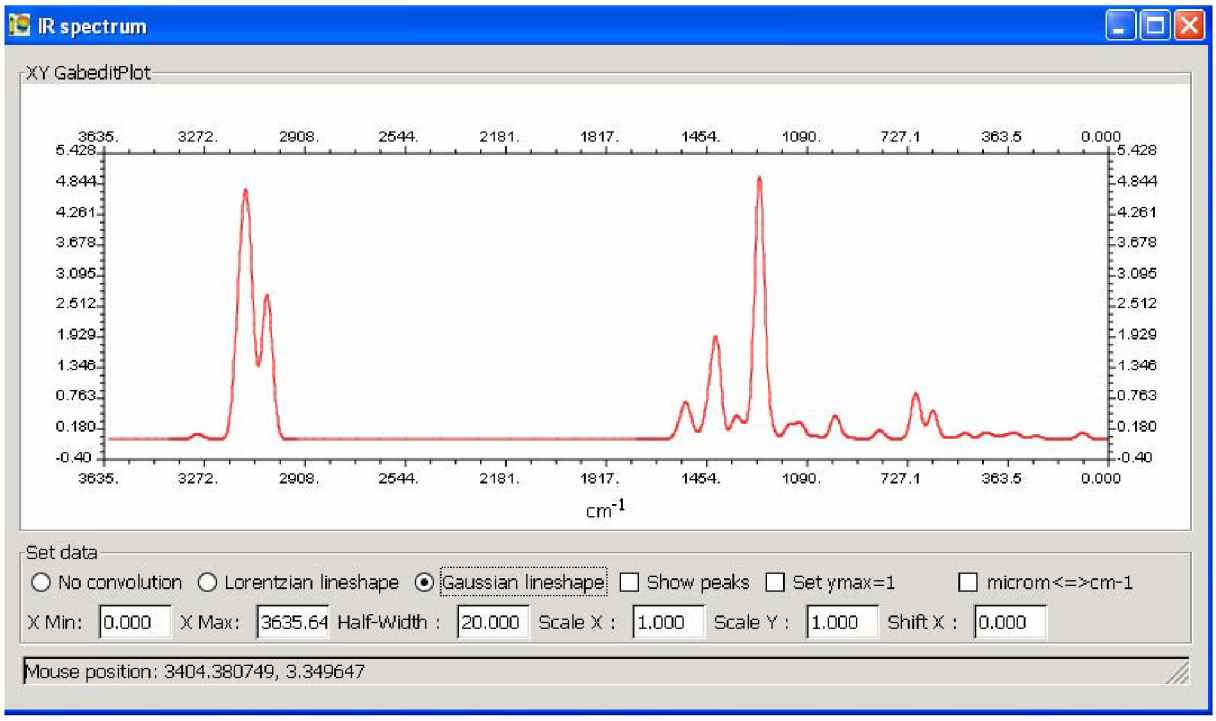

Fig. 28 The visualisation of IR spectrum in Gabedit

3 Experimental part

In our study we focused on 1,3-di-*terc*-butylimidazolium chloride **NC_1H-Cl,** 1,3-di-*terc*-butyl-imidazolinium chloride **NC_2H-Cl**, 1,3-di-*terc*-butylimidazol-2-ylidene **NC_1** and 1,3-di-*terc*-butylimidazolin-2-ylidene **NC_2** (Fig. 29) as representatives of N-heterocyclic carbene compounds. **NC_1H-Cl** was investigated as polymerization precursor in the Laboratory of Polymer Synthesis, BUT (Brno University of Technology), Faculty of Chemistry. This chloride precursor was purchased from Rhodia Company and was denote according to the provenience. Sample marked as FR from Lyon, France and sample marked as SH from Shanghai. "Free" carbene **NC_1** was prepared from **NC_1H-Cl**. Other compounds were investigated only by using computational studies, however the results obtained from the calculations were quit reasonable.

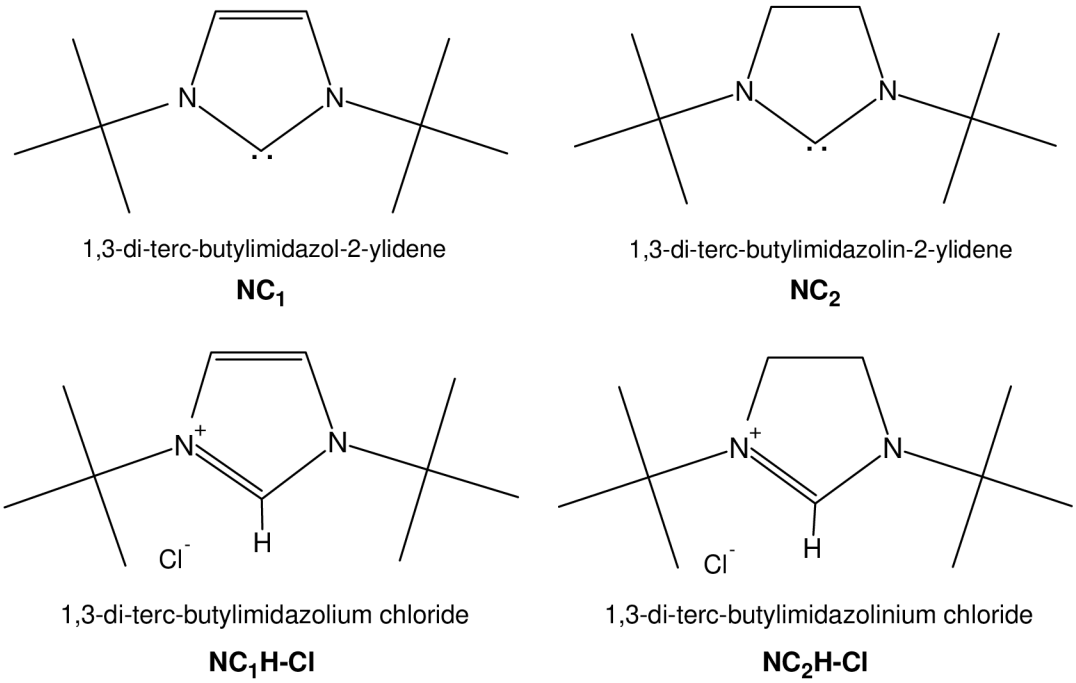

Fig. 29 Studied carbenes

First, some characteristics of studied molecules were determined using ArgusLab[43]. The energies and the symmetry of molecular orbitals were computed and electrostatic potential-mapped electron density surface were made (discussed in Section 2.7.8).

All molecules were first pre-optimized with the semi-empirical methods in ArgusLab[43] (discussed in Section 2.11.1). Then they were calculated with the RHF method using STO-6G, 6-31G, 6-31G*, 6-31+G, 6-311G and DZV basis sets and subsequently with the DFT (B3LYP functional) method using the same basis sets. These calculations were done in PC GAMESS/Firefly[41,42]. Energy gradients were calculated analytically with the optimization tolerance set to $1 \cdot 10^{-5}$ Hatree/Bohr. Since calculations on the computer were too slow (sometimes a number of days), the most calculations were continued on the BUT server pig.ro.vutbr.cz. Programs WinSCP[45] and PuTTy[46] were used for the manipulation on the server (discussed in Section 2.11.2).

Data of structural similar compounds, which have been already characterized, were obtained from CCDC (Cambridge Crystallographic Data Centre)[48,49,50,51]. Selected bond distances and bond angles of these compounds are given in Tab. 3. Predicted structures were compared with data from CCDC. Atoms were numbered in a way described in Fig. 30 to specify the bonds and angles.

Tab. 3 Selelected bond distances and bond angles obtained from CCDC

Compound	Bond distance (Å)					Bond angle (°)
	N(1)-C(1)	C(1)-N(2)	C(2)-C(3)	C(2)-N(1)	N(2)-C(3)	N(1)-C(2)-N(3)
NC_1	1.366(2)	1.366(2)	1.341(2)	1.380(2)	1.380(2)	102.19(12)
NC_1H-F_3CSO_3	1.336(5)	1.325(5)	1.345(5)	1.375(5)	1.378(5)	109.8(4)
NC_2	1.348(1)	1.347(1)	1.542(2)	1.476(1)	1.476(1)	106.44(9)
NC_2H-SCN	1.313(2)	1.314(2)	1.517(3)	1.473(2)	1.473(2)	113.80(16)

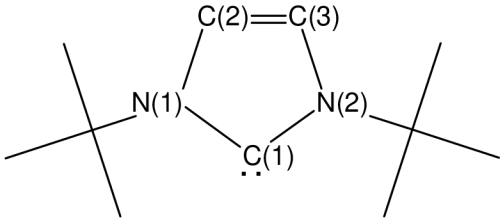

Fig. 30 The numbering of atoms

We had real IR spectra of NC_1H-Cl and of NC_1 measured on Bruker TENSOR 27 and RA spectra of NC_1H-Cl measured on Bruker EQUINOX IFS 55/S equipped with a Raman module FRA 106/S available. From data of geometry optimization IR and than RA intensities were obtained. Measured spectra were depicted in ACD/Spec Viewer[53] and set up in Excel[52]. Both measured and calculated spectra were compared. Moreover spectra of NC_1 were compared with the published ones.

4 Results and discussion

First, some characteristics of a molecule were determined to verify the behaviour of carbenes and their precursors. In ArgusLab[43] the energies of molecular orbitals were computed. It is well known that the symmetry and the energy of HOMO and LUMO have a significant influence on the mechanisms of reactions of molecules. The band gap represents the minimum energy which is essential for a realization of the transfer of an electron from the energy level HOMO to the energy level LUMO. Because of a small band gap both the studied carbenes are very reactive.

The visualization of selected molecular orbitals and electrostatic potential-mapped electron density surface were made. The representative example of the visualization is depicted in Fig. 31. The electron density surface gives the shape of the surface while the value of the electrostatic potential on this surface gives the colours. From the electrostatic potential-mapped electron density surface it is possible to notice that the electron density is bigger onto **NC_1** than onto **NC_2**. The increased electron density onto carbon atom observed in Fig. 32 is in an agreement with a premise that a lone pair is localized at a carbon atom. On the other hand the electron density in the carbene centre of **NC_1H-Cl** and **NC_2H-Cl** is lower which correlates is in an agreement with a premise that there is no lone pair in the carbene centre.

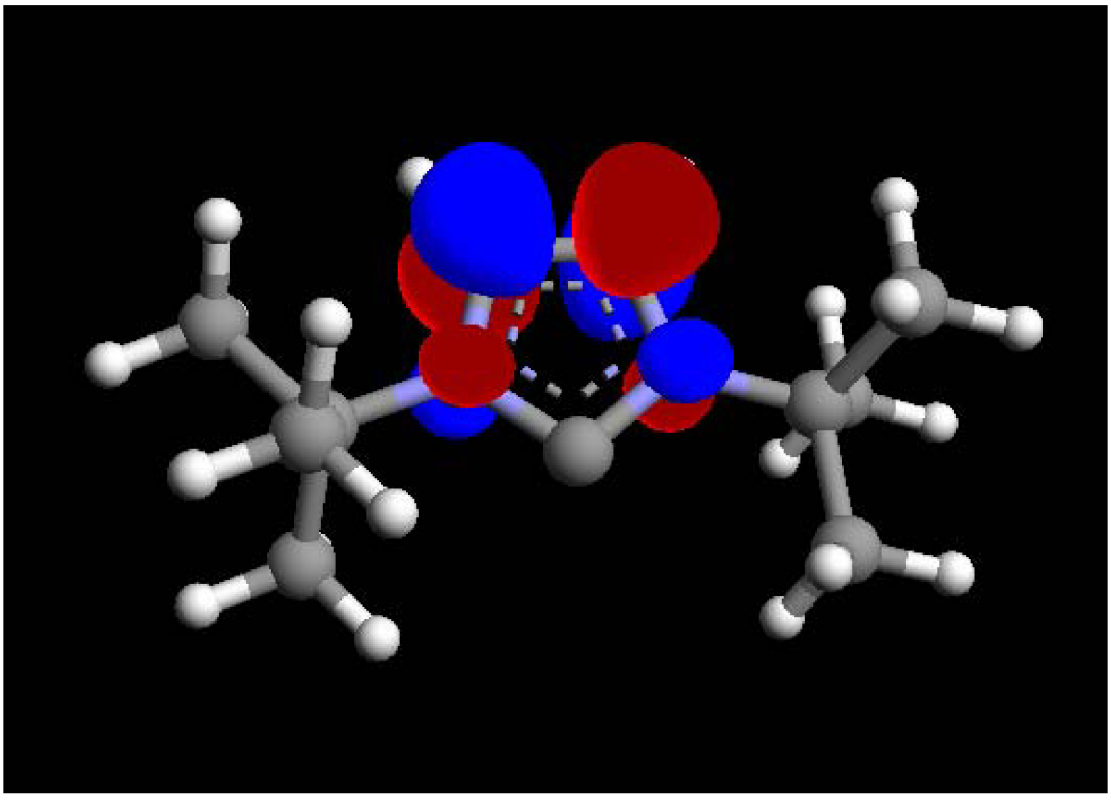

Fig. 31 The visualization of LUMO of NC_1 predicted by PC GAMESS/Firefly with RHF/6-31+G in ArgusLab

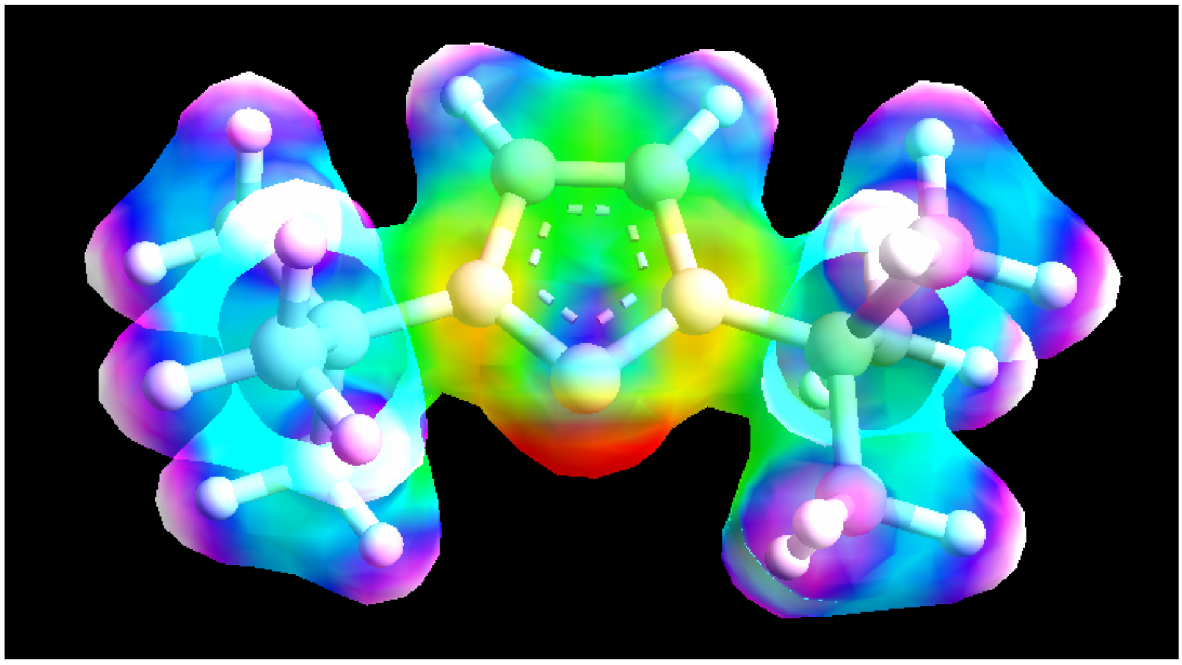

Fig. 32 The electrostatic potential-mapped electron density surface of NC_1 predicted by PC GAMESS/Firefly with RHF/6-31+G in ArgusLab

Data of bond distances and bond angles obtained by prediction by ArgusLab[43] differed from the data predicted by PC GAMESS/Firefly[41,42], therefore they were considered to be inaccurate. Selected bond distances and bond angles and average relative errors of **NC_1** and **NC_2** predicted by PC GAMESS/Firefly[41,42] with STO-6G bases set are summarized in Tab. 4. Selected bond distances and bond angles of **NC_1** predicted by PC GAMESS/Firefly[41,42] are summarized in Tab. 5, of **NC_1H-Cl** are summarized in Tab. 6, of **NC_2** are summarized in Tab. 7 and of **NC_2H-Cl** are summarized in Tab. 8. Moreover predicted structures of **NC_1** and **NC_2** were compared with data from CCDC, therefore Tab. 5 and Tab. 7 contain average relative errors **$E_\varnothing$**.

Tab. 4 Selected bond distances and bond angles predicted with STO-6G basis set

Compound	Bond distance (Å)					Bond angle (°)	$E_\varnothing$
	N(1)-C(1)	C(1)-N(2)	C(2)-C(3)	C(2)-N(1)	N(2)-C(3)	N(1)-C(2)-N(3)	(%)
NC_1	1.389	1.385	1.325	1.419	1.419	101.28	5.13
NC_1H-Cl	1.370	1.372	1.375	1.417	1.417	105.55	---
NC_2	1.374	1.372	1.562	1.469	1.467	108.69	1.92
NC_2H-Cl	1.361	1.358	1.530	1.504	1.507	108.47	---

It was confirmed that STO-6G basis set is deficient, so it is unfit for carbene compounds. Therefore this basis set was excluded from other tables.

Tab. 5 Selected bond distances and bond angles of NC_1

Basis set		Bond distance (Å)					Bond angle (°)	$E_{\varnothing}$
		N(1)-C(1)	C(1)-N(2)	C(2)-C(3)	C(2)-N(1)	N(2)-C(3)	N(1)-C(2)-N(3)	(%)
RHF	6-31G	1.367	1.364	1.337	1.398	1.397	103.38	0.70
	6-31G*	1.353	1.349	1.331	1.388	1.390	103.80	0.97
	6-31+G	1.367	1.362	1.339	1.396	1.398	103.63	0.73
	6-311G	1.365	1.361	1.335	1.396	1.398	103.66	0.80
	DZV	1.375	1.370	1.344	1.403	1.404	103.48	0.97
DFT	6-31G	1.387	1.383	1.361	1.405	1.407	102.19	1.34
	6-31G*	1.371	1.366	1.356	1.393	1.396	102.63	0.67
	6-31+G	1.386	1.382	1.362	1.407	1.407	102.56	1.41
	6-311G	1.383	1.380	1.356	1.404	1.407	102.59	1.25
	DZV	1.395	1.391	1.370	1.410	1.411	102.29	1.77

Tab. 6 Selected bond distances and bond angles of NC_1H-Cl

Basis set		Bond distance (Å)					Bond angle (°)
		N(1)-C(1)	C(1)-N(2)	C(2)-C(3)	C(2)-N(1)	N(2)-C(3)	N(1)-C(2)-N(3)
RHF	6-31G	1.329	1.329	1.346	1.389	1.390	109.41
	6-31G*	1.346	1.333	1.365	1.385	1.377	109.99
	6-31+G	1.312	1.336	1.351	1.381	1.388	110.21
	6-311G	1.327	1.328	1.343	1.388	1.388	109.52
	DZV	1.333	1.333	1.352	1.395	1.395	109.69
DFT	6-31G	1.351	1.350	1.368	1.398	1.397	108.35
	6-31G*	1.333	1.346	1.365	1.377	1.385	109.99
	6-31+G	1.352	1.352	1.370	1.397	1.397	108.35
	6-311G	1.349	1.349	1.365	1.397	1.397	108.53
	DZV	1.348	1.362	1.38	1.394	1.400	109.55

Tab. 7 Selected bond distances and bond angles of NC_2

Basis set		Bond distance (Å)					Bond angle (°)	$E_{\varnothing}$
		N(1)-C(1)	C(1)-N(2)	C(2)-C(3)	C(2)-N(1)	N(2)-C(3)	N(1)-C(2)-N(3)	(%)
RHF	6-31G	1.352	1.352	1.535	1.473	1.473	106.88	0.50
	6-31G*	1.342	1.343	1.523	1.462	1.461	107.03	0.66
	6-31+G	1.350	1.351	1.534	1.475	1.474	107.21	0.47
	6-311G	1.351	1.351	1.531	1.472	1.473	107.15	0.49
	DZV	1.360	1.360	1.539	1.481	1.480	106.98	0.79
DFT	6-31G	1.360	1.360	1.539	1.499	1.498	106.94	1.19
	6-31G*	1.352	1.352	1.531	1.483	1.483	106.74	0.53
	6-31+G	1.360	1.360	1.541	1.503	1.501	106.99	1.30
	6-311G	1.360	1.359	1.539	1.499	1.498	106.94	1.18
	DZV	1.370	1.370	1.544	1.504	1.505	106.61	1.58

Tab. 8 Selected bond distances and bond angles of NC_2H-Cl

Basis set		Bond distance (Å)					Bond angle (°)
		N(1)-C(1)	C(1)-N(2)	C(2)-C(3)	C(2)-N(1)	N(2)-C(3)	N(1)-C(2)-N(3)
RHF	6-31G	1.317	1.32	1.54	1.476	1.477	113.49
	6-31G*	1.312	1.312	1.532	1.464	1.465	113.95
	6-31+G	1.318	1.319	1.54	1.477	1.478	113.53
	6-311G	1.317	1.319	1.537	1.475	1.476	113.60
	DZV	1.322	1.323	1.548	1.481	1.482	114.13
DFT	6-31G	1.334	1.339	1.547	1.493	1.493	112.76
	6-31G*	1.328	1.331	1.539	1.477	1.48	113.22
	6-31+G	1.337	1.337	1.551	1.491	1.49	113.41
	6-311G	1.317	1.319	1.537	1.475	1.476	113.60
	DZV	1.348	1.349	1.557	1.491	1.49	113.07

Based on (Tab. 5) it was investigated, that the best results of NC_1 were obtained with DFT method using 6-31G* basis set. Generally, DFT methods were better than RHF methods for prediction **N(1)-C(2)-N(3)** bond angle, whereas RHF methods for prediction bond distance. Based on (Tab. 7) the similar trends were noticed. The best results of NC_2 were obtained with RHF method using 6-31+G basis set. According to these results following calculations were made with DFT method using 6-31G* basis set and with RHF method using 6-31+G.

Denk et al.[48] published computational study of NC_1 and NC_2 in 2001. The values of the same selected bond distances and bond angles of NC_1 displayed average relative errors of 1.02 %. On the other hand the same selected bond distances and bond angles of NC_2 contained average relative errors of 0.93 %. Based on these results, we can consider data predicted with RHF methods and with DFT/6-31G* to be in good agreement. However DFT methods should be better, because they involve electron correlation (Section 2.7.7).

The deviation could be the consequence of taking one isolated molecule in vacuum into account for the calculation. To reach a better accuracy using of the better method or the better basis set represents one of possible ways.

Up till now any structural data of compounds NC_1H-Cl or NC_2H-Cl have not been published yet. It was calculated that bonds **N(1)-C(1)**, **C(1)-N(2)**, **C(2)-N(1)** and **N(2)-C(3)** cut down against bonds of the appropriate carbenes, on the other hand the bond **C(2)-C(3)** elongated and the angle **N(1)-C(1)-N(2)** increased. Known data of similar precursors (Tab. 3) showed the same trends. Bonds **N(1)-C(1)** and **C(1)-N(2)** were shorter and the angle **N(1)-C(1)-N(2)** were bigger than bonds and angles of the appropriate carbenes.

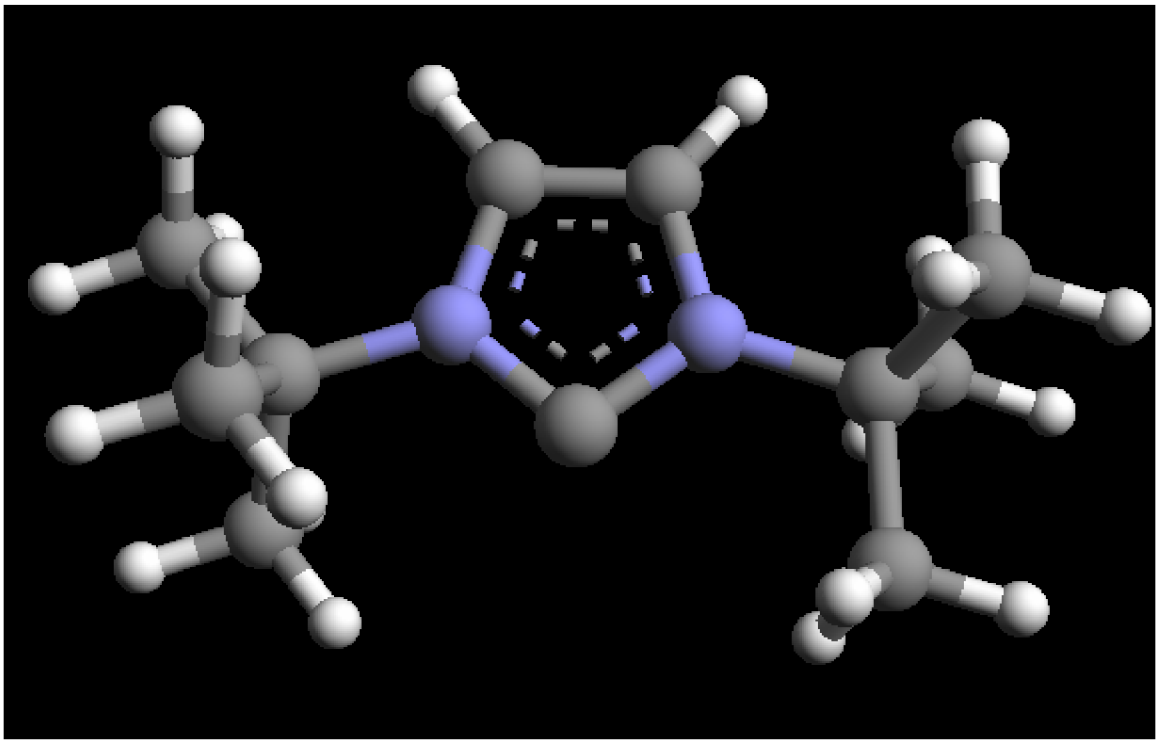

Fig. 33 The optimized structure of NC_1 predicted by PC GAMESS/Firefly with RHF/6-31+G in ArgusLab

From data of geometry optimization IR spectra (Fig. 34) and than RA spectra (Fig. 35) of **NC_1H-Cl** and IR spectra (Fig. 36) of **NC_1** were obtained. For the prediction of spectra RHF/6-31+G and DFT/6-31* methods were used. The infrared spectra (Fig. 34) predicted by using DFT/6-31* and RHF/6-31+G displayed the same character in the fingerprint region. These spectra were visualized in Gabedit[44] and converted into XY format. Spectra were set up in Excel[52].

The measured IR spectra of **NC_1H-Cl** are depicted in Fig. 37. Since the SH sample seemed to be purer than the FR sample its spectrum was taken for the comparison with the calculated one using with DFT/6-31* method (Fig. 38) (this method includes less systematic errors Section 2.10.4). The measured RA spectra of **NC_1H-Cl** are depicted in Fig. 39. These spectra had to be corrected due to the fluorescence of glass of the Schlenk flask. The measured spectrum (SH) was compared with calculated one using DFT/6-31* method (Fig. 40). Further, the measured IR spectra of NC_1 are depicted in Fig. 41. Measured spectra were depicted in ACD/Spec Viewer[53] and set up in Excel[52]. Intensities were marked according to Tab. 9.

Tab. 9 The notation of intensities

Intensity	Abbreviations
very strong	vs
strong	s
medium	m
weak	w
very weak	vw

Leites et al.[54] published measured and predicted spectra of $\mathbf{NC_1}$ in 2007. Thus we compared our measured spectra with that of Leites (Fig. 42). Intensities of IR spectra had to be converted due to the comparison into relative intensity according following conditions: intensity **vs** = 100, **s** = 80, **m** = 60, **w** = 40 and **vw** = 20. It was revealed, that compared spectra were not identical. It is well known that these compounds are stable only in the absence of oxygen and moisture[13] (Section 2.5). Thus our $\mathbf{NC_1}$ sample could hydrolyze. For the finding of the efficient cause next steps will be done.

The comparison between the Leites measured spectra and Leites predicted ones were done (Fig. 43) as well as between our measured spectra with Leites measured spectra were compared (Fig. 44). We did not found well correlation between predicted spectra and measured ones. The main reason was assuming one isolated molecule in gaseous phase for the prediction whereas for the measurement the compound in solid state was taken. To get deeper insight into this field further research will be done.

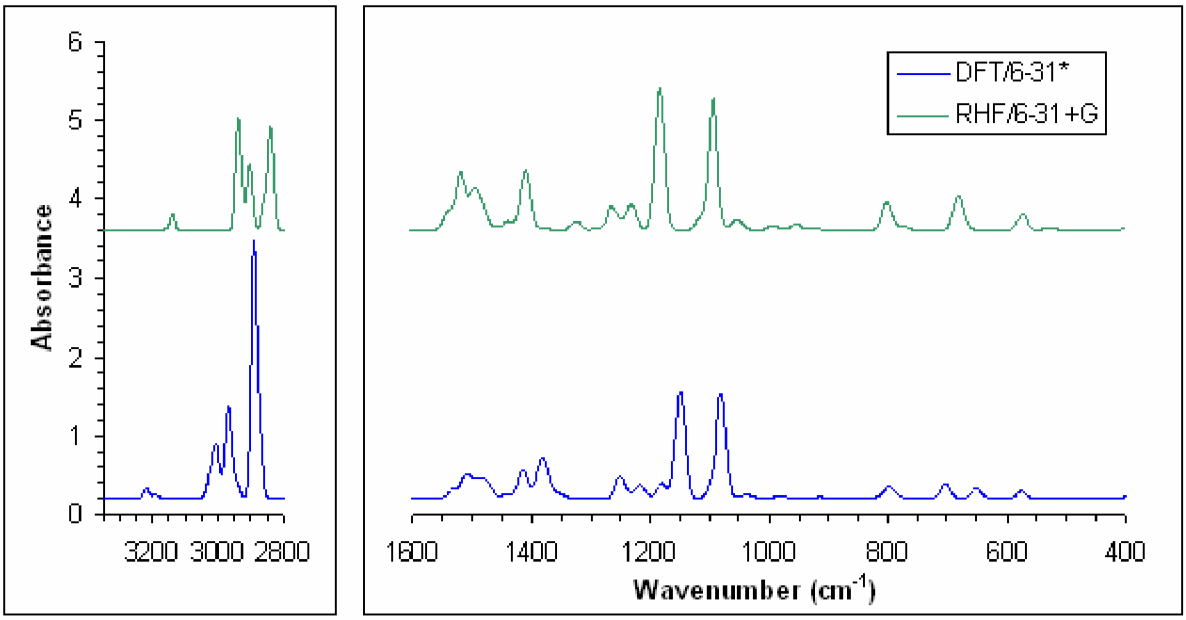

Fig. 34 Predicted IR spectra of NC_1H-Cl with DFT/6-31* ν (cm^{-1}): 573 (vw), 651 (vw), 677 (vw), 731 (vw), 799 (vw), 914 (vw), 982 (vw), 1037 (vw), 1081 (m), 1152 (m), 1180 (vw), 1217 (vw), 1252 (vw), 1383 (vw), 1415 (vw), 1490 (vw), 1508 (vw), 1532 (vw), 2892 (vs), 2967 (w), 3007 (w), 3219 (vw) and RHF/6-31+G ν (cm^{-1}): 523 (vw), 571 (vw), 678 (w), 799 (vw), 951 (vw), 992 (vw), 1051 (vw), 1092 (vs), 1182 (vs), 1227 (vw), 1263 (vw), 1322 (vw), 1405 (m), 1437 (vw), 1494 (w), 1517 (m), 2839 (s), 2905 (m), 2939 (s), 3143 (vw)

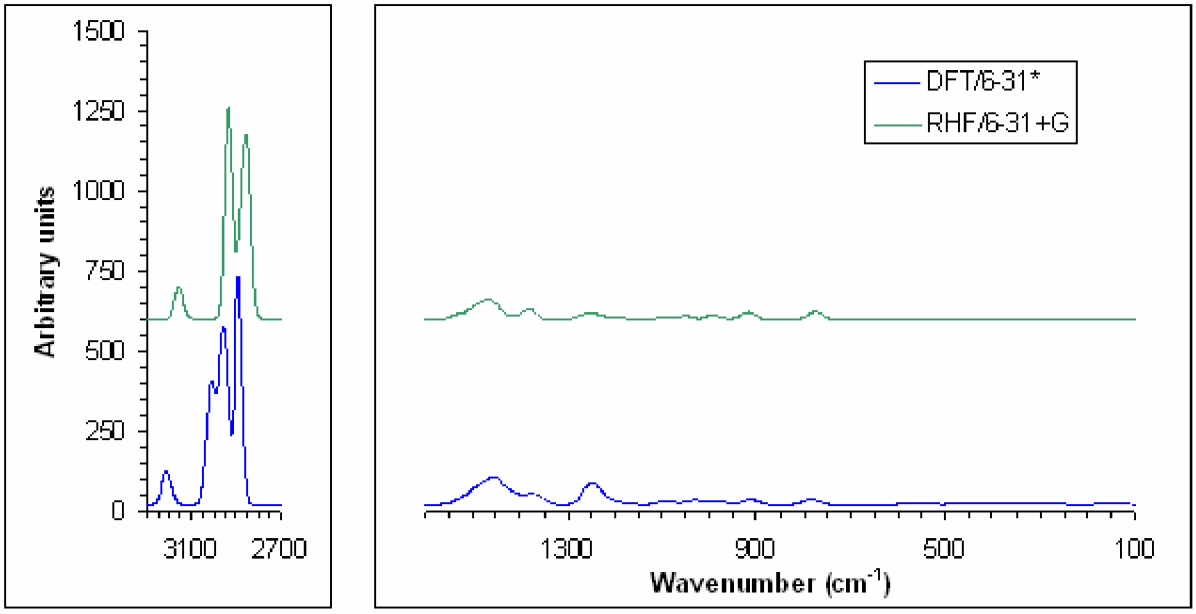

Fig. 35 Predicted RA spectra of NC_1H-Cl with DFT/6-31* ν (cm^{-1}): 278 (vw), 383 (vw), 577 (vw), 782 (vw), 907 (vw), 981 (vw), 1032 (vw), 1090 (vw), 1180 (vw), 1253 (vw), 1379 (vw), 1414 (vw), 1450 (vw), 1476 (vw), 1536 (vw), 2887 (vs), 2951 (m), 2963 (m), 3008 (w), 3192 (vw), 3219 (vw) and RHF/6-31+G ν (cm^{-1}): 275 (vw), 525 (vw), 570 (vw), 772 (vw), 917 (vw), 990 (vw), 1053 (vw), 1250 (vw), 1380 (vw), 1470 (vw), 2853 (vs), 2937 (vs), 3155 (vw)

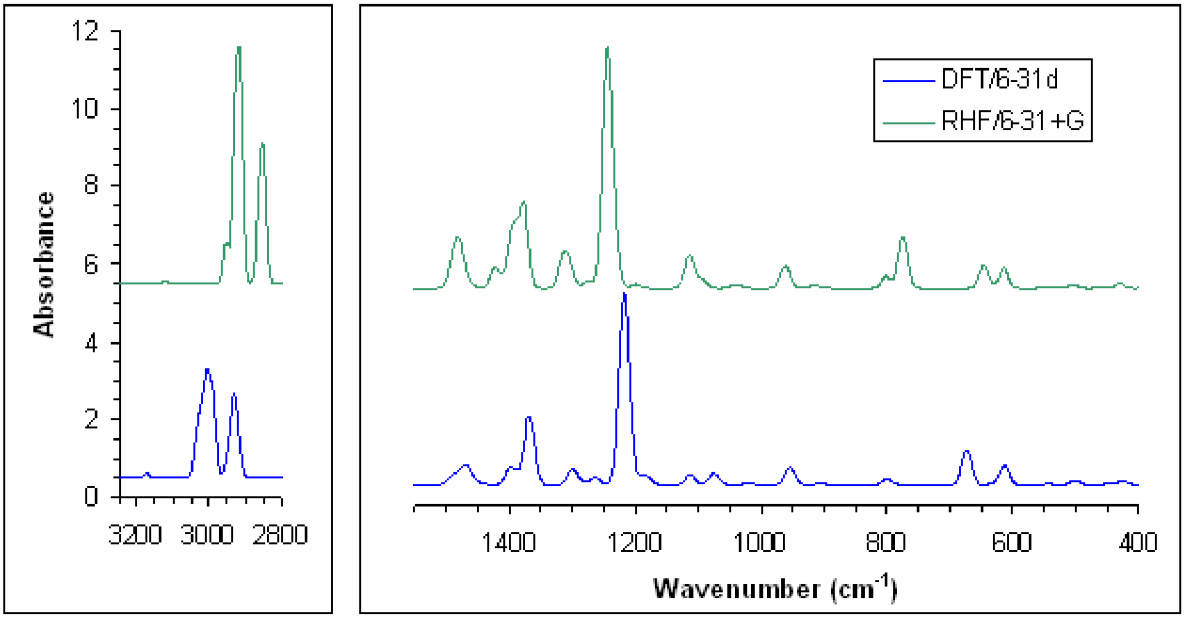

Fig. 36 Predicted IR spectra of NC_1 with DFT/6-31* ν (cm^{-1}): 425 (vw), 500 (vw), 546 (vw), 614 (vw), 673 (vw), 800 (vw), 907 (vw), 955 (vw), 1021 (vw), 1076 (vw), 1115 (vw), 1183 (vw), 1218 (s), 1265 (vw), 1301 (vw), 1366 (w), 1397 (vw), 1470 (vw), 2931 (m), 3009 (m), 3180 (vw) and RHF/6-31+G ν (cm^{-1}): 429 (vw), 505 (vw), 613 (vw), 648 (vw), 766 (vw), 802 (vw), 971 (vw), 1037 (vw), 1123 (vw), 1195 (vw), 1251 (vs), 1277 (vw), 1322 (vw),1379 (w), 1399 (w), 1425 (vw), 1486 (vw), 2855 (m), 2921 (vs), 3136 (vw)

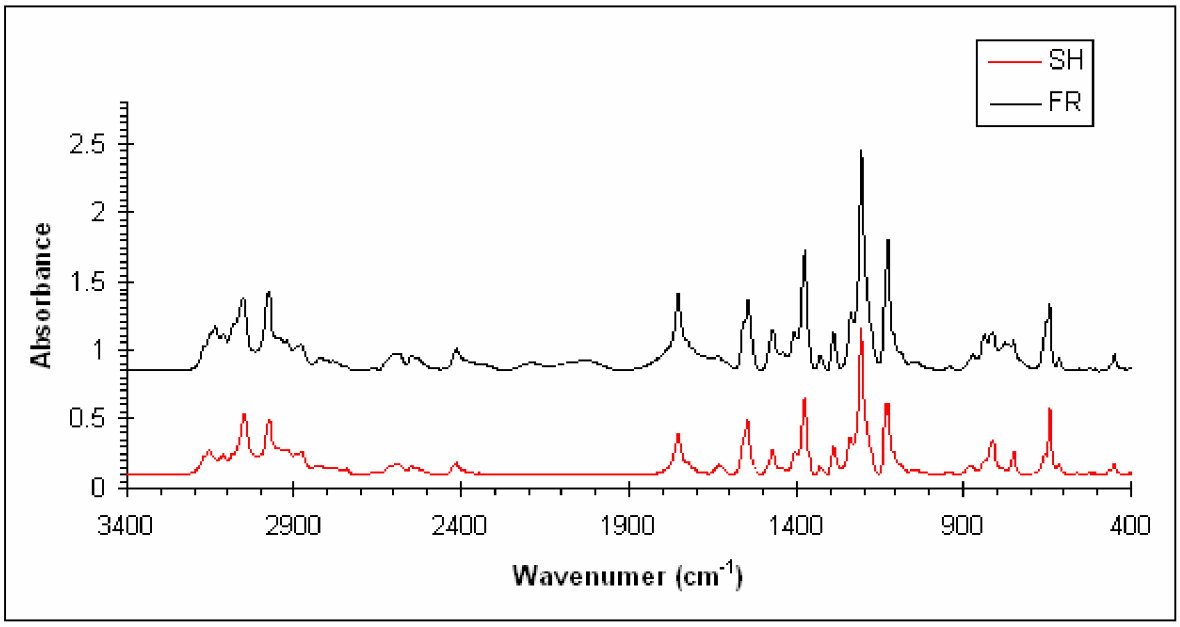

Fig. 37 The measured IR spectrum of NC_1H-Cl (FR) (Nujol, KBr) *v* (cm^{-1}): 451 (vw), 615 (vw), 642 (w), 654 (w), 750 (vw), 779 (vw), 810 (vw), 820 (vw), 839 (vw), 872 (vw), 1107 (vw), 1124 (m), 1207 (vs), 1238 (w), 1290 (vw), 1329 (vw), 1377 (m), 1408 (vw), 1441 (vw), 1472 (vw), 1545 (w), 1558 (w), 1632 (vw), 1753 (w), 2021 (vw), 2195 (vw), 2417 (vw), 2548 (vw), 2588 (vw), 2820 (vw), 2876 (vw), 2920 (vw), 2943 (vw), 2978 (w), 3055 (w), 3113 (vw), 3136 (W), 3171 (vw). The measured IR spectrum of NC_1H-C (SH) (Nujol, KBr) *v* (cm^{-1}): 401 (vw), 449 (vw), 615 (vw), 642 (m), 656 (vw), 750 (vw), 812 (w), 841 (vw), 874 (vw), 885 (vw), 1124 (m), 1132 (m), 1207 (vs), 1240 (w), 1290 (w), 1329 (vw), 1377 (m), 1406 (vw), 1441 (vw), 1474 (vw), 1547 (w), 1630 (vw), 1753 (w), 2417 (vw), 2548 (vw), 2588 (vw), 2876 (vw), 2920 (vw), 2976 (w), 3051 (m), 3113 (vw), 3154 (vw)

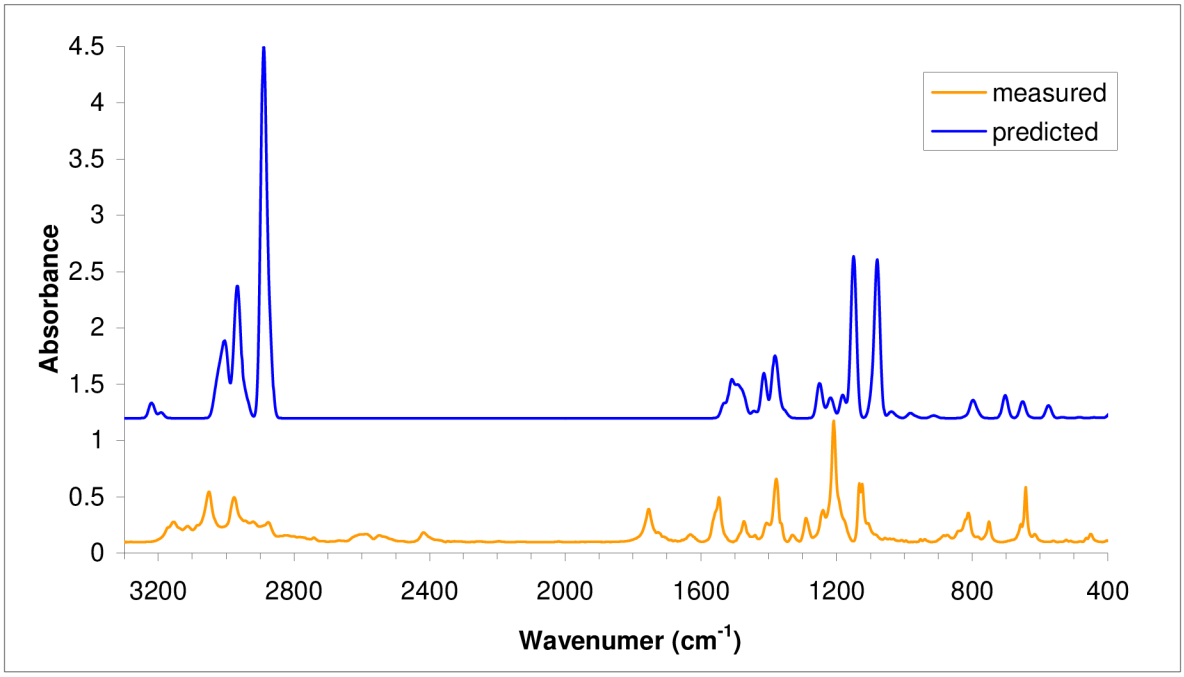

Fig. 38 The comparison of measured (SH) and predicted (DFT/6-31*) IR spectra of NC_1H-Cl

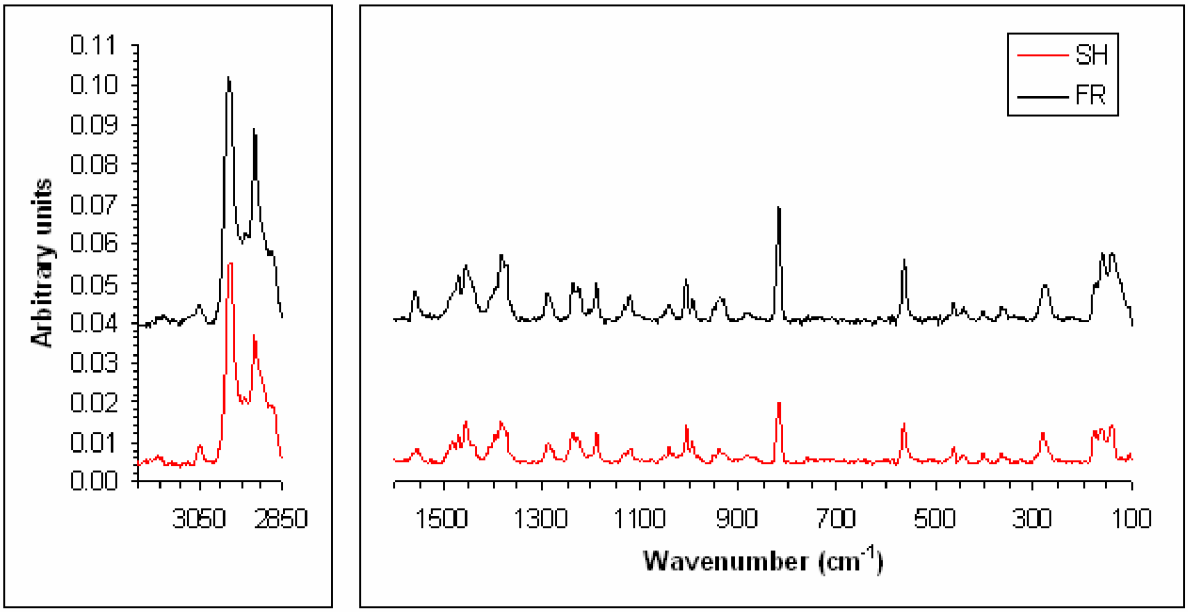

Fig. 39 The measured RA spectrum of NC_1H-Cl (FR) ν (cm^{-1}): 140 (w), 157 (w), 278 (vw), 367 (vw), 464 (vw), 562 (vw), 818 (vw), 937 (vw), 995 (vw), 1007 (vw), 1040 (vw), 1123 (vw), 1189 (vw), 1237 (vw), 1290 (vw), 1385 (w), 1455 (w), 1469 (vw), 1558 (w), 2736 (vw), 2803 (vw), 2981 (vs), 3051 (vw), 3141 (vw). The measured RA spectrum of NC_1H-Cl (SH) ν (cm^{-1}): 140 (vw), 159 (vw), 174 (vw), 280 (vw), 367 (vw), 403 (vw), 463 (vw), 563 (vw), 817 (w), 941 (vw), 996 (vw), 1007 (vw), 1042 (vw), 1121 (vw), 1188 (vw), 1238 (vw), 1383 (vw), 1455 (vw), 1469 (vw), 1481 (vw), 1555 (vw), 2731 (vw), 2801 (vw), 2917 (s), 2976 (vs), 3048 (vw), 3154 (vw)

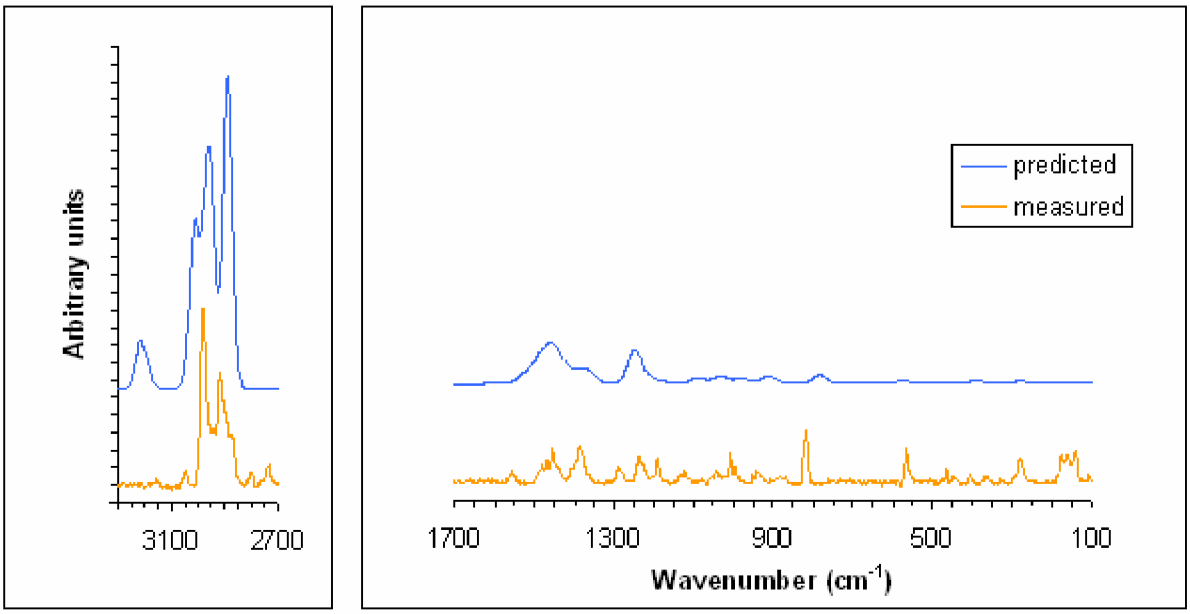

Fig. 40 The comparison of measured (SH) and predicted (DFT/6-31*) RA spectra of NC_1H-Cl

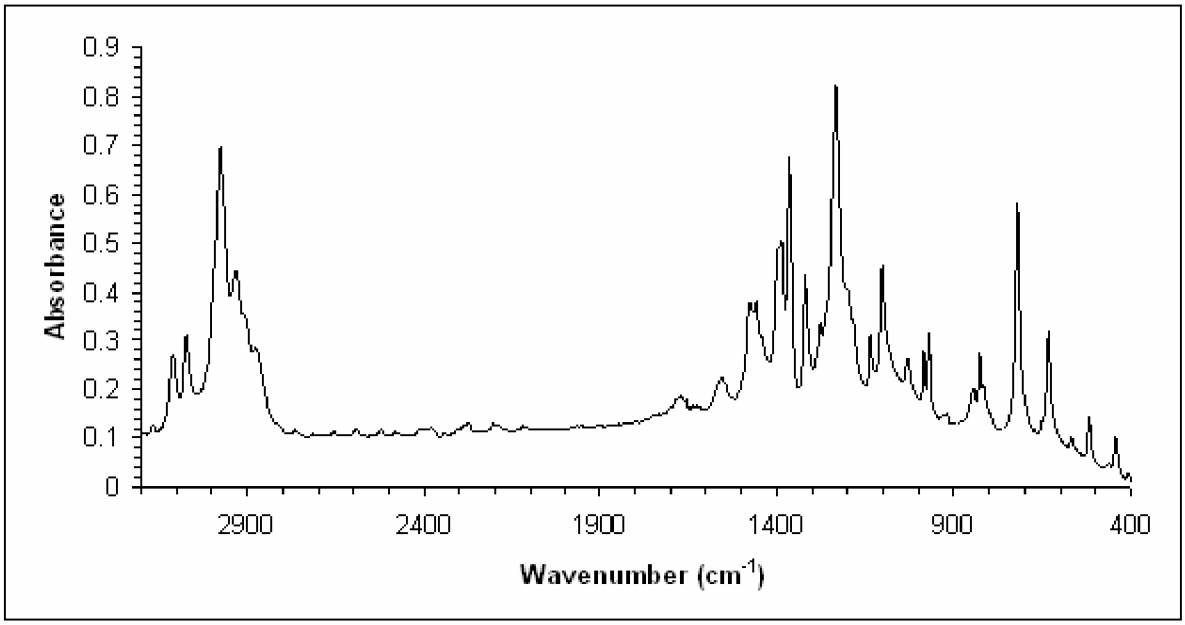

Fig. 41 The measured IR spectrum of NC_1 (Nujol, KBr) ν (cm^{-1}): 444 (vw), 519 (vw), 567 (vw), 633(w), 719 (s), 816 (w), 827 (w), 847 (w), 922 (vw), 970 (w), 986 (w), 1031 (w), 1101 (m), 1136 (w), 1202 (m), 1234 (vs), 1277 (m), 1319 (m), 1366 (vs), 1387 (s), 1458 (m), 1476 (m), 1555 (w), 1657 (w), 1672 (w), 1686 (w), 2876 (w), 2909 (m), 2932 (m), 2976 (vs), 3073 (w), 3109 (w)

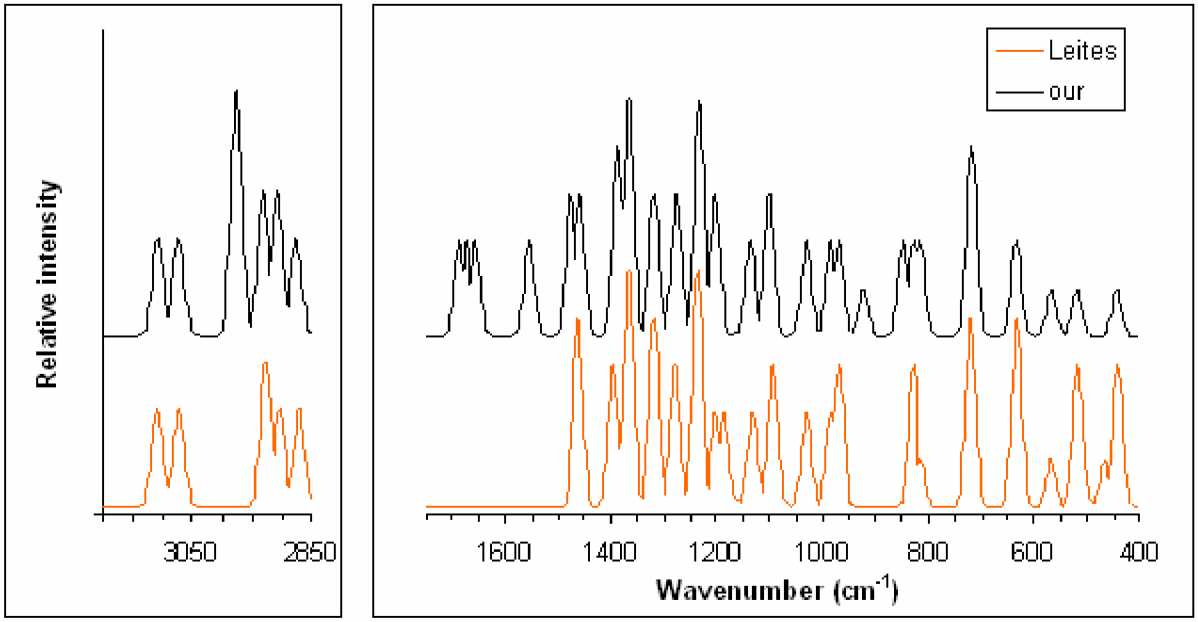

Fig. 42 The comparison of measured spectra of NC_1

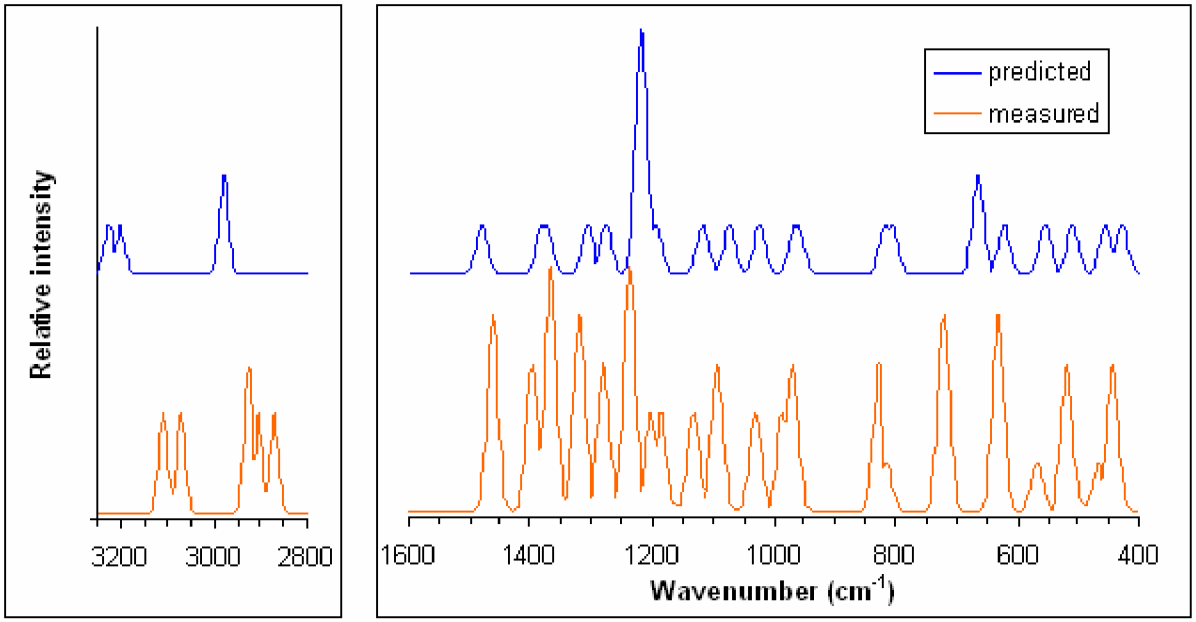

Fig. 43 The comparison of Leites measured and predicted spectra

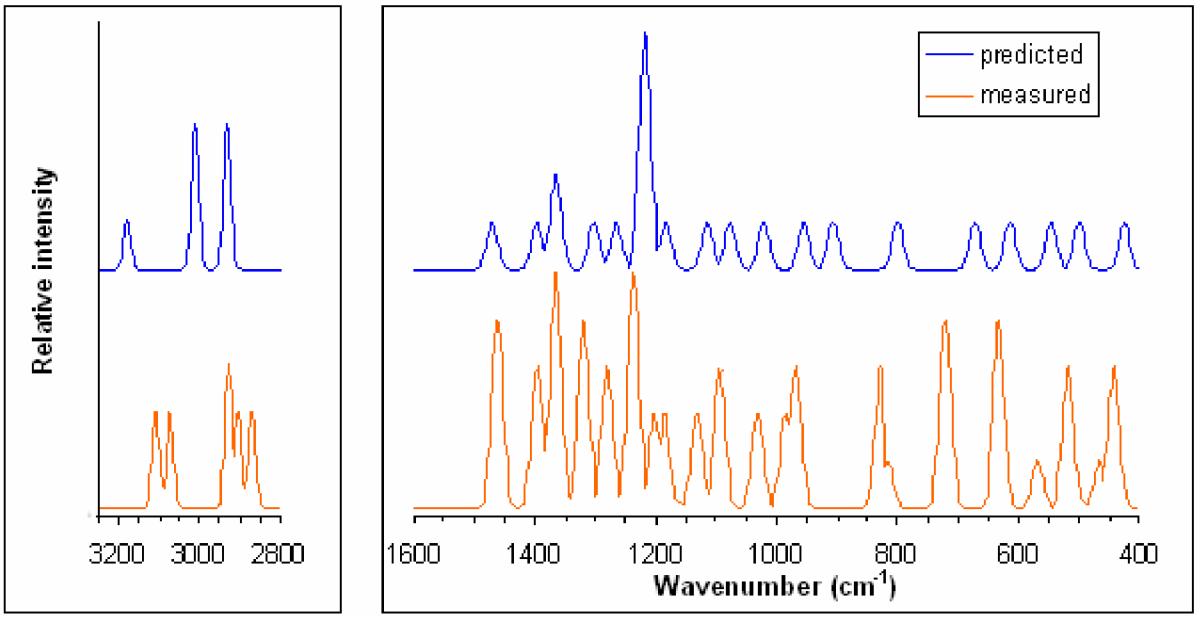

Fig. 44 The comparison between Leites measured spectra and our predicted spectra

5 Conclusion

In ArgusLab[43] the energies of molecular orbitals of selected N-heterocyclic carbenes and their precursors based on chlorides were computed and the visualization of selected molecular orbitals and electrostatic potential-mapped electron density surface were made. These calculations are essential for the prediction of properties. Both the studied carbenes are very reactive because of a small band gap of these energies. The influence of substituents on the gap of these energies will be the subject for further study, eventually the better catalysts will be proposed.

In PC GAMESS/Firefly[41,42] the geometry optimization of selected N-heterocyclic carbenes and their precursors based on chlorides was made and best method and basis set were found. Four compounds were calcutated with two methods using the same five basis sets. The calculated structures were in good agreement with the published data. In next steps methods including electron correlation effect in addition will be studied.

It was proved, that changes of bond distances and bond angles of precursors based on chlorides against appropriate carbenes shows the same trends as the other analogical systems.

From data of geometry optimization IR and than RA spectra of selected imidazole compounds were obtained. Subsequently, calculated spectra with measured ones were compared. To get deeper insight into this field further research will be done.

The make of geometry optimization and findings of selected characteristics of molecules were the aim of our work. Obtained data from geometry optimization will be used for further calculations. The finding of the efficient cause for the prediction of IR and RA spectra and subsequently their interpretation, eventually the obtaining of NMR spectra will be the subject for further study.

6 References

[1] *Molecular Electronic Structure* [online]. 2001 [ref. 2010-04-20]. Available from: <http://www.chm.bris.ac.uk/pt/harvey/elstruct/introduction.html#menu>.

[2] Greenwood, N., Earnshaw, A.: *Chemistry of the Elements*. 2nd ed. Oxford: Butterworth-Heinemann, 1997. 1341 p. ISBN 0-7506-3365-4.

[3] Yamaguchi, T., Yamamoto, Y., Kinoshita, D., Akiba, K., Zhang, Y., Reed, C. A., Hashizume, D., Iwasaki, F.: Synthesis and Structure of a Hexacoordinate Carbon Compound. Journal of the American Chemical Society. 2008, vol. 130, p. 6894-6895.

[4] Minkin, V. I., Minyaev R. M.: Hypercoordinate carbon in polyherdal organic structures. *Mendeleev Communications*. 2004, vol. 14(2), p. 43-46.

[5] Yamashita, M., Yamamoto, Y., Akiba, K., Hashizume, D., Iwasaki, F., Takagi, N., Nagase, S.: Syntheses and Structures of Hypervalent Pentacoordinate Carbon and Boron Compounds Bearing an Anthracene Skeleton – Elucidation of Hypervalent Interaction Based on X-ray Analysis and DFT Calculation. *Journal of the American Chemical Society*. 2005, vol. 127, p. 4354-4371.

[6] Akiba, K., Moriyama, Y., Mizozoe, M., Inohara, H., Nishi, T., Yamamoto, Y., Minoura, M., Hashizume, D., Iwasaki, F., Takagi, N., Ishimura, K., Nagase, S.: Synthesis and Characterization of Stable Hypervalent Carbon Compounds (10-C-5) Bearing a 2,6-Bis(*p*-substituted phenyloxymethyl)benzene Ligand. *Journal of the American Chemical Society*. 2005, vol. 127, p. 5893-5901.

[7] Carilla, J., Fajarí, L., Juliá, L.: (2,6-Dichlorophenyl)bis(2,4,6-trichlorophenyl)methyl Radical. Synthesis, Magnetic Behaviour aand Crystal Structure. *Tetrahedron*. 1996, vol. 52, p. 7013-7024.

[8] Herrmann, W. A., Köcher C.: N-Heterocyclic Carbenes. *Angewandte Chemie International Edition in English*. 1997, vol. 35, p. 2162-2187.

[9] Skell, P. S., Sandler, S. R.: Reactions of 1,1-dihalocyclopropanes with Electrophilic Reagents. Synthetic Route for Inserting a Carbon Atom between the Atoms of a Double Bond. *Journal of the American Chemical Society*. 1958, vol. 80, p. 2024.

[10] Fischer, E. O., Maastaböi, A.: On the Existence of a Tungsten Carbonyl Carbene Complex. *Angewandte Chemie International Edition in English*. 1964, vol. 3, p. 580-581.

[11] Brookhart, M., Studabaker, W. B.: Cyclopropanes from Reactions of Transition-Metal-Carbene Complexes with Olefins. *Chemical Reviews*. 1987, vol. 87, p. 411-432.

[12] Wanzlick, H.-W., Schikora, E.: Ein neuer Zugang zur Carben-Chemie. *Angewandte Chemie*. 1960, vol. 70, p. 494.

[13] Arduengo, A. J. III, Harlow, R. L., Kline, M.: A Stable Crystalline Carbene. *Journal of the American Chemical Society*. 1991, vol. 113, p. 361-363.

[14] Bourissou, D., Guerret, O., Gabbaï, P., Bertrand, G.: Stable Carbenes. *Chemical Reviews*. 2000, vol. 100, p. 39-91.

[15] Schuster, G. B.: Structure and Reactivity of Carbenes having Aryl Substituents. *Advences in Physical Organic Chemistry*. 1986, vol. 22, p. 311-361.

[16] Gleiter, R., Hoffmann, R.: Stabilizing a singlet methylene. *Journal of the American Chemical Society*. 1968, vol. 90, p. 5457-5460.

[17] *IUPAC Gold Book* [online]. c2005-2009 [ref. 2010-04-09]. Available from: <http://goldbook.iupac.org/index.html>.

[18] McMurry, J.: *Organic Chemistry*. 6rd ed. California: Brooks/Cole, a Thompson Learning Company, 2004. 1376 p. ISBN 0534389996.
[19] Harrison, J. F: Electronic Structure of Carbenes. I. Methylene, fluoromethylene, and difluoromethylene. *Journal of the American Chemical Society*.1971, vol. 93, p. 4112-4119.
[20] Hoffmann, R., Zeiss, G. D., Van Dine, G. W.: The Electronic Structure of Methylenes. *Journal of the American Chemical Society*. 1968, vol. 90, p. 1485-1499.
[21] Moss, R. A., Wlostowski, M., Shen, S., Krogh-Jespersen, K., Matro, A.: Dimethoxycarbene: Direct Observation of an Archetypal Nucleophilic Carbene. *Journal of the American Chemical Society*. 1988, vol. 110, p. 4443-4444.
[22] Schoeller, W. W.: When is a Singlet Carbene Linear? *Journal of the Chemical Society - Chemical Communications*. 1980, p. 124-125.
[23] Gilbert, B. C., Griller, D., Nazran, A. S.: Structures of Diarylcarbenes and Their Effect on the Energy Separation between Singlet and Triplet States. *Journal of Organic Chemistry*. 1985, vol. 50, p. 4738-4742.
[24] Arduengo, A. J. III: Looking for Stable Carbenes: The Difficulty in Starting Anew. *Accounts of Chemical Research*. 1999, vol. 32, p. 913-919.
[25] Arduengo, A. J. III, Bock, H., Chen, H., Denk, M., Dixon, D. A., Green, J. C, Herrmann, W. A., Jones, N. L., Wagner, M., West, R.: Photoelectron Spectroscopy of a Carbene/Silene/Germylene Series. *Journal of the American Chemical Society*. 1994, vol. 116, p. 6641-6649.
[26] Heinemann, C., Müller, T., Apeloig, Y., Schwarz, H.: On the Question of Stability, Conjugation, and "Aromacity" in Imidazol-2-ylidenes and Their Silicon Analogs. *Journal of the American Chemical Society*. 1996, vol. 118, p. 2023-2038.
[27] Teles, J. H., Melder, J.-P., Ebel, K., Schneider, R., Gehrer, E., Harder, W., Brode, S., Enders, D., Breuer, K., Raabe, G.: The Chemistry of Stable Carbenes: Benzoin-Type Condensations of Formaldehyde Catalyzed by Stable Carbenes. *Helvetica Chimica Acta*. 1996, vol. 79, p. 61-83.
[28] Enders, D., Breuer, K., Teles, J. H.: A Novel Asymmetric Benzoin Reaction Catalyzed by a Chiral Triazolium Salt. Preliminary communication . *Helvetica Chimica Acta*. 1996, vol. 79, p. 1217-1221.
[29] Kamber, N. E., Jeong, W., Gonzalez, S., Hendrick, J. L., Waymouth, R. M.: N-Heterocyclic Carbenes for the Organocatalytic Ring-Opening Polymerization of ε-Caprolactone. Macromolecules. 2009, vol. 49, p. 1634-1639.
[30] *The Chemogenesis Web Book*: *Lewis Acids and Lewis Bases* [online]. c1999-2009 [ref. 2010-05-03]. Available from: <http://www.meta-synthesis.com/webbook/12_lab/lab.html>.
[31] Pearson, R. G.: Hard and Soft Acids and Bases. *Journal of the American Chemical Society*. 1963, vol. 85, p. 3533-3539.
[32] *IUPAC, Glosary of terms used in theoretical organic chemistry:* Hard and Soft Acid and Base (HSAB) principle [online]. 2006 [ref. 2010-04-09]. Available from: <http://old.iupac.org/reports/1999/7110minkin/h.html>.
[33] Leach, A. R.: *Molecular Modelling: Principles and Application*. 2nd ed. Harlow: Pearson Education Limited, 2001. 744 p. ISBN 0-582-38210-6.
[34] Foresman, J. B., Frisch, AE.: *Exploring Chemistry with Electronic Structure Methods*. 2nd ed. Pittsburgh, PA: Gaussian, Inc., 1996. li, 302 p. ISBN 0-9636769-3-8.

[35] Szabo, A., Ostlund, N. S.: *Modern quantum chemistry*. 3nd ed. New York: Dover Publications, Inc., 1996. 466 p. ISBN 0—69186-1.

[36] Boys, S. F.: Electronic Wave functions. I. AGeneral Method of Calculation for the Stationary States of Any Molecular System. *Proceedings of the Royal Society of London. Series A, Mathematical and Physical Sciences*. 1950, vol. 200, p. 542-554.

[37] *Firefly (former PC GAMESS) Homepage* [online]. 1999 [ref. 2009-11-12]. Available from: <http://classic.chem.msu.su/gran/gamess/index.html>

[38] Nakamoto, K.: *Infrared and Raman Spectra of Inorganic and Coordination Compounds, Part A: Theory and Applications in Inorganic Chemistry*. 6th ed. Hoboken, New Yersey: John Wiley & Sons, Inc., 2009, 419 p. ISBN 978-0-471-74339-2.

[39] *Virtual Textbook of Organic Chemistry: Infrared spectroscopy* [online]. 1999 [ref. 2010-05-01]. Available from: <http://www.cem.msu.edu/~reusch/VirtualText/Spectrpy/InfraRed/infrared.htm#ir1>.

[40] Merrick, J. P., Moran, D., Radom, L.: An Evaluation of Harmonic Vibrational Frequency Scale Factors. *Journal of Physical Chemistry A*. 2007, vol. 111, p. 11683-11700.

[41] Granovsky, A. A. *PC GAMESS/Firefly version 7.1.F* [computer program]. 2005 [ref. 2009-5-20]. Available from: <http://classic.chem.msu.su/gran/gamess/index.html>.

[42] Schmidt, M. W., Baldridge, K. K., Boatz, J. A., Elbert, S. T., Gordon, M. S., Jensen, J. H., Koseki, S., Matsunaga, N., Nguyen, K. A., Su, S., Windus, T. L., Dupuis, M., Montgomery, A. J.: General atomic and molecular electronic structure system. *Journal of Computational Chemistry*. 1993, vol. 14, is. 11, 1347-1363.

[43] *ArgusLab 4.0.1*. [computer program]. 1996 [ref. 2009-04-24]. Available from: <http://www.arguslab.com/index.htm>.

[44] *Gabedit 2.2.8* [computer program]. 2002 [ref. 2010-01-28]. Available from: <http://gabedit.sourceforge.net/>.

[45] *PuTTY 0.60* [computer program]. c1997-2007 [ref. 2010-02-25]. Available from: <http://www.chiark.greenend.org.uk/~sgtatham/putty/download.html>.

[46] *WinSCP 4.2.5*. [computer program]. c2000-2009 [2010-02-15]. Available from: <http://winscp.net/eng/download.php>.

[47] RUNpcg [computer program]. 2008 [ref. 2009-5-20]. Available from: <http://www.chemsoft.ch/qc/RUNpcg.htm>.

[48] Denk, M. K., Rodezno, J. M., Gupta, S., Lough, A. J. Synthesis and reactivity of subvalent compounds: Part 11. Oxidation, hydrogenation and hydrolysis of stable diamino carbenes. *Journal of Organometallic Chemistry*. 2001, vol. 617-618, p. 242-253.

[49] Rijnberg, E., Richter, B., Thiele, K. H., Boersma J., Veldman, N., Spek, A. L., Koten, G. A Homologous Series of Homoleptic Zinc Bis(1,4-di-*tert*-butyl-1,4-diaza-1,3-butadiene) Complexes: K_x[Zn(*t*-BuNCHCHN-*t*-Bu)$_2$], Zn(*t*-BuNCHCHN-*t*-Bu)$_2$, and [Zn(*t*-BuNCHCHN-*t*-Bu)$_2$](OTf)$_x$ (x = 1, 2). *Inorganic Chemistry*. 1998, vol. 37, p. 56-63.

[50] Denk, M. K., Thadani, A., Hatano, K., Lough, A. J. Sterisch gehinderte stabile nucleophile Carbene. *Angewandte Chemie*. 1997, vol. 109, p. 2719-2721.

[51] Denk, M. K., Gupta, S., Brownie, J., Tajammul, S., Lough, A. J. C-H Activation with Elemental Sulfur: Synthesis of Cyclic Thioureas from Formaldehyde Aminals and S_8. *Chemistry - A European. Journal*. 2001, vol. 7, p. 4477-4486.

[52] *Microsoft Excel 2003* [computer program]. c1985-2001 [ref. 2007-04-27].
[53] *ACD/Spec Viewer 4.53* [computer program]. c1997-2000 [ref. 2009-11-21]. Available from: < http://www.acdlabs.com/home/>.
[54] Leites, L. A., Magdanurov, G. I., Bukalov, S. S., Nolan, S. P., Scott, N. M., West, R.: Vibrational and electronic spectra and the electronic structure of an unsaturated Arduengo-type carbene. *Mendeleev Communications*. 2007, vol. 17, p. 92-94.

7 List of abbreviations

2c-2e	Two-centre two-electron bond
3c-2e	Three-centre two-electron bond
3c-4e	Three-centre four-electron bond
CC	Coupled cluster
CCDC	Cambridge crystallographic data centre
DFT	Density functional theory
DZV	Double zeta valence
FTP	File transfer protocol
GAMESS	General atomic and molecular electronic structure system
GTO	Gaussian type orbital
HOMO	Highest occupied molecular orbital
HSAB	Hard and soft acid and bases
IR	Infrared
LCAO	Linear combination of atomic orbitals
LUMO	Lowest unoccupied molecular orbital
M	Spin multiplicity
MCSCF	Multi-configurational self-consistent field
MP	Møller-Plesset Pertubation theory
MRDCI	Multireference single and double configuration interaction
NC_1	1,3-di-*terc*-butylimidazol-2-ylidene
NC_2	1,3-di-*terc*-butylimidazolin-2-ylidene
NC_1H-Cl	1,3-di-*terc*-butylimidazolium chloride
NC_2H-Cl	1,3-di-*terc*-butylimidazolinium chloride
NEVPT	N-elecron valence state pertubation theory
QCI	Quadratic configuration interaction
RA	Raman
RHF	Restricted Hartree Fock
ROHF	Restricted open shell Hartree Fock
SCF	Self-consistent field
SFTP	Secure file transfer protocol
SSH	Secure shell
STO	Slater type orbital
TCP	Transmission control protocol
THF	Tetrahydrofurane
UHF	Unrestricted Hartree Fock